Abundance–diversity relationship as a unique signature of temporal scaling in the fossil record

Published Version:
Tomašových, A., Kowalewski, M., Nawrot, R., Scarponi, D., Zuschin, M. (2024). Abundance–diversity relationship as a unique signature of temporal scaling in the fossil record. ECOLOGY LETTERS, 27(7), 1-15 [10.1111/ele.14470].

Availability:
This version is available at: https://hdl.handle.net/11585/995285 since: 2024-10-31

Published:
DOI: http://doi.org/10.1111/ele.14470

Abundance-diversity relationship as a unique signature of temporal scaling in the fossil record

Adam Tomašových[1]*, Michał Kowalewski[2], Rafał Nawrot[3], Daniele Scarponi[4], Martin Zuschin[3]

[1]Earth Science Institute, Slovak Academy of Sciences, 84005, Bratislava, Slovakia, ORCID: 0000-0002-0471-9480

[2]Florida Museum of Natural History, University of Florida, 1659 Museum Road, Gainesville, FL, ORCID: 0000-0002-8575-4711

[3]Department of Palaeontology, University of Vienna, Josef-Holaubek-Platz 2, 1090 Vienna, Austria, ORCID: 0000-0002-5774-7311, 0000-0002-5235-0198

[4]Dipartimento di Scienze Biologiche, Geologiche e Ambientali, University of Bologna, Via Zamboni 67, 40126 Bologna, Italy, ORCID: 0000-0001-5914-4947

*Corresponding author: Adam Tomašových, geoltoma@savba.sk

Keywords: paleoecology, macroecology, species diversity, species-time relationship, Holocene, time averaging

Author Contributions: A.T, M.K., R.N., D.S. and M.Z. designed research, collected data, and performed analyses; A.T wrote the initial draft, and A.T, M.K., R.N., D.S. and M.Z. contributed to the final version.

Competing Interest Statement: The authors declare no competing interest.

Running title: Temporal scaling of fossil-record diversity

Abstract: 149 words

Main Text: 5126 words

Number of figures: 6

Number of references: 81

Supporting text

Figures S1-S11

Tables S1-S5 (separate files)

SI references

Data files and scripts at Dryad-Zenodo: https://doi.org/10.5061/dryad.fttdz0903 https://doi.org/10.5281/zenodo.11664933

Abstract

Species diversity increases with the temporal grain of samples according to the species-time relationship, impacting paleoecological analyses because the temporal grain (time averaging) of fossil assemblages varies by several orders of magnitude. We predict a positive relation between total abundance and sample size-independent diversity (ADR) in fossil assemblages because an increase in time averaging, determined by a decreasing sediment accumulation, should increase abundance and depress species dominance. We demonstrate that, in contrast to negative ADR of non-averaged living assemblages, the ADR of Holocene fossil assemblages is positive, unconditionally or when conditioned on the energy availability gradient. However, the positive fossil ADR disappears when conditioned on sediment accumulation, demonstrating that ADR is a signature of diversity scaling induced by variable time averaging. Conditioning ADR on sediment accumulation can identify and remove the scaling effect caused by time averaging, providing an avenue for unbiased biodiversity comparisons across space and time.

INTRODUCTION

In recent years, ecologists have become increasingly interested in biodiversity dynamics across timescales, achieving new insights through the integration of neo- and paleoecological data (Buma et al. 2019; Benito et al. 2020; Pandolfi et al. 2020; Patrick et al. 2021; Dornelas et al. 2023; Rillo et al. 2022). However, differences in temporal grain of fossil assemblages and their consequences for diversity patterns need to be accounted for to avoid invalid inferences (Powell and Kowalewski 2002; Bush and Bambach 2004; Balseiro and Waisfeld 2014; Carlucci and Westrop 2015; Finnegan et al. 2019). Species diversity increases with the temporal grain of samples as predicted by eco-evolutionary models and observed in neoecological and paleoecological time series according to the species-time relationship (STR, Figure 1, Preston 1960, Rosenzweig 1998). Temporal grain of paleoecological samples is equal to time averaging that corresponds to the cumulative amount of time during which the individuals forming a fossil assemblage have lived (Kidwell 2013). Estimates of species diversity thus depend on the time span over which a given assemblage is observed in neoecological surveys (Adler and Lauenroth 2003; Fridley et al. 2006; Castillo-Escrivà et al. 2020; O'Sullivan et al. 2021) or over which it is incorporated into the stratigraphic record (Scarponi and Kowalewski 2007; Tomašových and Kidwell 2010a). As marine and terrestrial environments are characterized by variability in sediment accumulation rate, in disintegration rate of organismal (typically skeletal) remains, and in their mixing by burrowers (Aller 1982; Kidwell 1986), time averaging of fossil assemblages in a single paleoecological time series can vary by several orders of magnitude, from years or decades to multiple millennia or longer (Scarponi et al. 2013; Tomašových et al. 2016; Ritter et al. 2023). This large variability in time averaging magnifies the importance of the scaling effect generated by the STR in paleoecological, as opposed to neoecological time series, in which the temporal grain of sampling units can be directly controlled.

In contrast to neoecological data, estimation of time averaging is challenging in the fossil record as the accuracy of geochronological tools is limited. Fluctuations in diversity observed in the fossil record across series of assemblages, which slide up and down along the STR continuum according to their time averaging, can be thus difficult to distinguish from changes driven by eco-evolutionary processes. To address this problem, here we formulate a simple prediction regarding the effect of the variability in temporal grain on the diversity observed in the fossil record. This prediction, which ultimately can be used to filter out scaling effects on diversity, postulates that the relation between the total fossil abundance and diversity estimated with methods that remove its dependency on sample size (ADR; Hurlbert 1971; Chao et al. 2014, 2020) will be pulled towards positive values in fossil assemblages (Figure 2). This prediction relies on the negative effect of *sediment accumulation rate* on both (1) the abundance of fossils (total abundance of individuals standardized to sediment mass or volume) and (2) the time averaging of fossil assemblages themselves, which influences the shape of the species-abundance distribution (Figure 2A, Tomašových and Kidwell 2010b) and thus species diversity (Šizling et al. 2009; Alroy 2015; Chase et al. 2018; McGlinn et al. 2021).

First, in the absence of variability in sedimentation and disintegration, fossil abundance is a function of both standing abundance and mortality of living populations that eventually enter as dead individuals into the sediment (Figure 2A). Fossil abundance integrates this flux of dead individuals into historical layers over variable durations of time averaging. A decrease in sediment accumulation rate (i.e., in the input of non-skeletal sediment) will increase the abundance of individuals in fossil assemblages (Kidwell 1986). Although fossil abundance is also reduced by disintegration rate (Figure 2A), this prediction is supported empirically as fossil concentrations are associated with stratigraphic surfaces that result from reduced accumulation rates (Kidwell 1989; Abbott 1997; Egenhoff and Maletz 2007). Second, although the time averaging of fossil assemblages will decline with skeletal disintegration and will increase with mixing (Figure 2A), the sediment accumulation rate is a first-order control of time averaging in most settings (Scarponi et al. 2013; Tomašových et al. 2023). Therefore, species diversity of assemblages, measured with indices that are independent of sample size or use sample size-based or coverage-based rarefaction, will increase with declining sediment accumulation rate as species dominance and the slope of the rank-abundance distribution decline with increasing time averaging (steep gray solid lines scale to flatter dashed lines, right column in Figure 1). This prediction primarily applies to taxa with high preservation potential in the fossil record (such as calcareous foraminifers, ostracods or molluscs).

Here, we evaluate whether the abundance-diversity relation in fossil assemblages (ADR_F) in the Holocene record of molluscs in the northern Adriatic Sea is positive, unconditionally or when conditioned on the energy availability gradient (i.e., water depth), and thus whether it carries the signature of variable time averaging. The abundance-diversity relation independently documented in living assemblages (ADR_L) provides a benchmark for abundance and diversity not affected by time averaging that can be compared with the ADR_F observed in the fossil record. Based on 26 age-dated sediment cores, we assess the hypotheses positing (1) that sediment accumulation covaries negatively with fossil abundance and species diversity, (2) that fossil abundance and species diversity are positively related, either unconditionally or when conditioned by the energy availability that shapes the ADR_L in the northern Adriatic Sea (Figure 2B-I), and (3) are independent when conditioned on sediment accumulation (Figure 2J-M). To determine whether our findings apply to other taxa, we assess the ADR_L and ADR_F in marine benthic foraminiferal assemblages from different areas worldwide using data from the Biodeeptime database (Smith et al. 2023).

CONCEPTUAL FRAMEWORK: PREDICTIONS FROM SPECIES-TIME RELATIONSHIP INDEPENDENT OF SAMPLE SIZE

The STR is assessed in terms of how the raw species richness increases as a function of accumulation of temporally-segregated samples. In this approach, diversity increases not only as a function of increasing temporal grain (time averaging) but also as a function of increasing sample size. This effect leads to the positive slope of the STR even when the increase in diversity is driven purely by sampling. Although the contribution of sampling to the STR slope can be segregated from the ecological processes that induce temporal turnover in species composition (White et al. 2004, 2006), the STRs can be assessed on the basis of a sample-size independent diversity, i.e., the Hill-transformed probability of interspecific encounter (PIE). In Figure 1, we summarize the scaling of this measure as a function of increasing time averaging in two distinct dispersal-limited metacommunity models. They differ in the degree of niche equivalence and density-dependence but nevertheless generate positive STRs by changing the shape of rank-abundance distributions as a consequence of increasing time averaging. On the one hand, species have equal demographic rates on a per capita basis in a neutral model, leading to steady-state diversity and an evolving metacommunity species pool in drift-speciation equilibrium (following Hubbell 2001). On the other hand, species differ in density-independent niche breadth (standard deviation of the Gaussian response equal to 0.1 and 0.5 relative to the gradient length of one) and the strength of interspecific competitive interactions (α_{ij} = 0.5 or 0.95, relative to intraspecific α_{ii} of 1) in non-neutral models with constant metacommunity richness (following Thompson et al. 2020).

Figure 1 visualizes the model predictions under these scenarios (source scripts in R Core Team (2021) in the Supplement). Namely, the increase in diversity is associated with the decline in species dominance and the flattening of rank-abundance distributions (e.g., reducing its slope when fitted by the geometric, power-law or power-bend distributions), with rank abundance distributions of non-averaged assemblages (1 year) being steeper than those of assemblages time-averaged to 1,000 years. The ADR_F is predicted to mimic the species-time relationships because the total abundance is proportional to the product of standing abundance and the inverse of lifespan, with abundance along the x-axis stretched or squeezed depending on the lifespan of organisms.

The Hill-transformed diversity based on PIE should remain constant with increasing time averaging only when local assemblages represent random samples from a static metacommunity pool (sampling model of Coleman, 1981) or from an evolving metacommunity pool sampled over time spans that are shorter than the time scale of metacommunity diversification (e.g., over 1,000 years when the mean time of species originating in a metacommunity is 10,000 years, black lines in Figure 1A). This scenario is captured by the neutral model and thus can occur when species extinctions due to ecological drift are in equilibrium with speciation (Hubbell 2001; McGill et al. 2005). The STR slope will be positive in all other scenarios, determined by processes such as density dependence, dispersal limitation, or turnover related to habitat filtering (White et al. 2006; Carey et al. 2007; McGlinn and Palmer 2009; Raia et al. 2011). Once the scale of time averaging approaches the time scale of metacommunity diversification, even randomly assembled metacommunities will exhibit a positive ADR_F. The estimates of diversity independent of sample size (such as the diversity based on PIE) or standardized to the same sampling completeness (Alroy 2010, Chao et al. 2020) will thus invariably increase with increasing time averaging. This scaling effect does not necessarily increase the evenness measures that have species richness in the denominator as the sensitivity of these indices to time averaging depends on the ratio of higher-order diversity relative to species richness.

The theoretical predictions visualized in Figure 1 and in the path diagrams in Figure 2 provide a framework for interpreting the empirical ADR_F. The ADR can be measured in the logarithmic space as a regression coefficient specifying the effect of logged abundance on logged diversity or as a Pearson correlation coefficient between these variables (empirical species-time relations tend to be power law-like, White et al. 2006). The effects of increasing time averaging that pulls the ADR_F towards positive values can be visualized in cartoons depicting the abundance-diversity space and path diagrams in Figure 2. These cartoons assume that assemblages are subjected to random time averaging that varies by four orders of magnitude, that the scaling exponent for the Hill-transformed PIE-based diversity is 0.1, and that the individual lifespan is one year. The abundance and diversity will be positively related in fossil assemblages varying in time averaging if abundance is unrelated to diversity in living assemblages (Figure 2B). However, when standing abundance and diversity exhibit a nonrandom relationship in living assemblages (Chase and Leibold 2002; Storch et al. 2018), the resulting ADR_F is a combination of (1) ecological processes driving the ADR_L (e.g., energy or resource availability affecting both variables at yearly or generational scales) and (2) STR scaling effects (Figure 2B-D). Conditioning the ADR_F on the gradient in energy availability that forces the positive or negative ADR_L will lead to the positive ADR_F if the scaling STR effects contribute to variability in diversity (Figure 2F-H). Therefore, the positive ADR_F, either unconditional or conditioned on the energy availability gradient, can be a criterion for detecting variability in diversity induced by variability in time averaging in the fossil record. However, the effect of temporal scaling can be confirmed by conditioning the ADR_F on sediment accumulation: if this conditioning leads to the independency between fossil abundance and diversity, the variability in diversity is likely truly triggered by variability in time averaging (Figure 2J-L). Finally, conditioning the ADR_F on sediment accumulation only can be used to infer the original ADR_L as determined by ecological processes unrelated to temporal scaling.

MATERIAL AND METHODS

Study system – macrofaunal assemblages in the Adriatic Sea. The northern Adriatic Sea is one of the few regions where both living assemblages and age-dated, volume-standardized fossil assemblages were extensively sampled at the scale of the whole basin. We compiled information on the total standing abundance and diversity of living molluscan communities from published surveys performed in the late 20th and early 21st century at water depths between intertidal and 70 m (Figure S1). This dataset includes 1,150 living assemblage samples represented by Van Veen grabs (0.1 m^2) or sediments from 1 m^2 quadrats collected by scuba divers (Table S1). Data on 489 molluscan fossil samples were compiled from 26 sediment cores collected in the northern Adriatic Sea and Po coastal plain and documented in our former studies (Table S2). Eleven 1-1.5 m-long piston and gravity cores were collected at 12-44 m water depth (Gallmetzer et al. 2016). These cores were split into 4-5 cm-thick increments; assemblages from all increments were surveyed. Fifteen cores (> 10 m-long) from the Po coastal plain were split into 5 and 10-cm increments sampled either at 1-3 m intervals or more densely in the case of frequent facies shifts. Age data for 26 cores were compiled from the original reports (at least 6 dated levels per core or at least 2 dated levels per systems tract, Figures S2-S3) and analyzed with Bayesian age-depth models (Blaauw and Christen 2011) to compute variability in estimates of sediment accumulation rate (cm/y) (see Supporting Information, Figure S4-S5).

***Living and fossil macrofaunal assemblages*.** In all compiled studies, samples of living and fossil molluscan assemblages were all sieved with a 1 mm mesh size. The abundance of living molluscan individuals was standardized to 1 m^2. The fossil abundance was estimated as the total number of all identifiable molluscan specimens based on exhaustive counting of all specimens in each increment, or by extrapolating to the total increment volume from sample splits, and splits standardized to the number of specimens per 1 dm^3 of sediment. Species diversity was estimated as the Hill-transformed PIE (Hsieh et al. 2016). The minimum raw (unstandardized) sample size is 10 individuals and the median sample size is 139 individuals.

Water depth was measured for living assemblages during sampling and indirectly estimated for fossil assemblages based on a compositional gradient in non-metric multidimensional scaling (NMDS). The first axis of NMDS based on the Chord distances and the proportional abundances of molluscan species orders the Holocene fossil assemblages along a bathymetric gradient (Figure S6-S7), as documented in former studies (e.g., Wittmer et al. 2014). To visualize differences in total abundance and diversity between living and fossil assemblages, we partition living assemblages (shallower and deeper than 10 m) and fossil assemblages (two main groups detected by a cluster analysis based on the same abundance data, Figure S8) into two equivalent, onshore (sandy intertidal and fluvially-influenced nearshore) and offshore (muddy offshore transition and distal prodelta) segments.

***Abundance-diversity relationship in macrofaunal assemblages*.** We estimate regression coefficients specifying the effect of abundance on diversity using the linear mixed-effect models (all variables normalized to z-scores). The effect of fossil abundance on fossil diversity (ADR_F) will vary not only as a function of time averaging but also as a function of ecological variables (such as energy or resource availability) that jointly affect standing abundance and diversity of living assemblages (ADR_L, Figure 2B-D). We use water depth as such a variable as it affects the diversity and standing abundance of benthic invertebrates (Tumbiolo and Downing 1994; Cusson and Bourget 2005). Water depth can also covary with sediment accumulation and thus can confound the effects of sediment accumulation on fossil diversity or abundance. The effect of water depth is thus partialled out in the assessment of the two hypotheses postulating that sediment accumulation reduces diversity and abundance of fossil assemblages. We then assess the corollaries that correspond to three levels of conditioning (three rows in Figure 2): (1) ADR_F is unconditionally positive, (2) ADR_F is positive when conditioned on an energy availability gradient; and (3) ADR_F disappears when the effect of sediment accumulation on ADR_F is partialled out. The third level is equal to a structural equation model that finds that the model that incorporates the effect of abundance on diversity is not better than the model where the covariance between abundance and diversity is set to zero.

To estimate the effect of abundance on diversity, we use the linear mixed-effect models that account for heterogeneity among cores (with random intercepts and slopes) and within-core temporal autocorrelations (with a covariate represented by a stratigraphic depth and the within-core correlation structure modelled by the autoregressive process of order 1, using the nlme package, Pinheiro et al. 2023). The variation in sediment accumulation, abundance, and diversity is markedly smaller within cores than among cores (Figure S9), and the majority of cores in offshore environments were deposited under slow net sediment accumulation. Therefore, the fixed effects covary with random effects, violating the assumption of the mixed-effect models. We thus partitioned the fixed effects into within and between-core effects of abundance and sediment accumulation on diversity in these models (van de Pol and Wright 2009). Although this approach increases the number of parameters, the between-core effect of abundance on diversity can be expected to mirror the scaling effect when time averaging varies primarily among cores. Finally, we use generalized additive models to visualize the shape of the dependency of abundance and diversity on water depth and a two-line test to assess whether this dependency along the whole bathymetric gradient is U-shaped (Simonsohn 2018). We transformed fossil abundance, diversity, and sediment accumulation to natural logarithms as the empirically documented STRs tend to be approximately linear in the logarithmic space (White et al. 2006) and such transformation also reduces the skewness of residuals.

Abundance-diversity relationship in microfaunal living and fossil assemblages. To assess the ADR_L and ADR_F in another clade, we compiled from the literature (1) 30 surveys of abundance and diversity in living benthic foraminifers (Table S3); and (2) 73 surveys of abundance and diversity in fossil benthic foraminifers in Holocene-Pleistocene cores, using the Biodeeptime database (Smith et al. 2023). We restricted the data to surveys with at least 10 samples with volume- or mass-standardized counts per geographic region or per time series (Table S4). We quantified the ADR_L in 30 regions and the ADR_F at the scale of (1) individual cores (73 series) and (2) at the scale of larger regions that consist of at least two cores (25 series). As the ADR_L is based on modern spatial surveys whereas the ADR_F is assessed on the basis of spatio-temporal stratigraphic record, we use a simple Pearson correlation to compare the ADR_L and ADR_F of microfaunal assemblages (generalized least-squares accounting for temporal autocorrelation led to similar results). All data are available at https://doi.org/10.5061/dryad.fttdz0903 and R language scripts at https://doi.org/10.5281/zenodo.11664933.

RESULTS

Effects of sediment accumulation on macrofaunal abundance and diversity. Sediment accumulation in the northern Adriatic Sea declines from ~10 cm/y in onshore deltaic environments to only ~0.001 cm/y at offshore locations. As predicted, fossil abundance is affected negatively by sediment accumulation when water depth (energy availability) is partialled out in mixed-effect models ($\beta = -0.18$, $p < 0.0001$, Figure 3A, Table 1). Similarly, fossil diversity is negatively affected by sediment accumulation in mixed-effect models ($\beta = -0.18$, $p < 0.0001$, Figure 3D). Although molluscan abundance declines with water depth in living assemblages ($\beta = -0.47$, $p < 0.0001$, Figure 3B), fossil abundance is invariant to water depth ($\beta = 0.02$, $p = 0.37$, Figure 3C). The PIE-based diversity increases with water depth in both living ($\beta = 0.3$, $p < 0.0001$, Figure 3E) and fossil assemblages ($\beta = 0.33$, $p = <0.0001$, Figure 3F).

Macrofaunal abundance-diversity relation. The ADR_L is negative ($\beta = -1.17$, $p < 0.0001$, $\beta_{depth} = -0.7$, $p < 0.0001$, Figure 4A). In contrast, the unconditional ADR_F is generally positive ($\beta = 0.72$, $p = 0.03$) but rather complex, U-or V-shaped (two-line test with a breakpoint at diversity = 1.9 separates a negative segment from a positive segment, with $p < 0.05$). The two maxima in fossil abundance correspond to (1) almost monospecific assemblages in onshore environments and (2) diverse assemblages in offshore environments (Figure 4B). The linear mixed-effect model shows that the between-core effect of abundance on diversity is positive when conditioned on water depth ($\beta_{depth} = 0.73$, $p < 0.0001$, Figure 4C) whereas the within-core abundance effect on diversity is negative ($\beta_{depth} = -0.023$, $p = 0.029$). This contrast between among-core and within-core abundance effects on diversity is striking when analyses are limited to offshore environments ($\beta_{between} = 0.33$, $p < 0.\ 001$, $\beta_{within} = -0.11$, $p = 0.001$, Figure 4D). The unconditional ADR_F is thus a composite of two patterns: the fossil diversity does not systematically change with abundance in onshore environments ($\beta = 0.61$, $p = 0.66$, light gray points in Figure 5A), whereas it increases with abundance in offshore environments ($\beta = 0.99$, $p < 0.0001$, light gray points in Figure 5B), ascending in parallel with increasing time averaging (contours in Figure 5B).

Macrofaunal abundance-diversity relation conditioned by sediment accumulation. The *positive* effect of between-core abundance on diversity in mixed-effect models disappears when conditioned on sediment accumulation ($\beta = 0.11$, $p = 0.77$, $\beta_{depth} = 0.15$, $p = 0.4$). The within-core abundance has weak negative effects on diversity ($\beta=-0.025$, $p = 0.08$, $\beta_{depth} = -0.03$, $p = 0.029$, Table 1). Given that the effect of abundance on diversity is not positive and that the AIC of the full model that includes the effect of fossil abundance on fossil diversity (AIC = -3244.6) is only 1.9 units smaller than the AIC of the model that does not incorporate this effect (AIC = -3242.7), the positive relation between the abundance and diversity of fossil assemblages is accounted for by the confounding effect of sediment accumulation (Table 1).

Microfaunal abundance-diversity relation. ADR_L does not show any preference for positive values (median $r = -0.18$), with six datasets exhibiting a significantly negative ADR_L and two datasets (7%) exhibiting a significantly positive ADR_L (Figure 6, Table S3). 30% of 73 Holocene-Pleistocene cores exhibit a significantly positive (unconditional) ADR_F (median $r = 0.08$, Figure 6, Table S4). This estimate also incorporates environments with low variability in sediment accumulation where the positive ADR_F is not expected to develop, and thus the danger of misattributing the observed diversity fluctuations to ecological processes rather than to the scaling effects is low. When the analyses are restricted to the cores with high variability in time averaging and abundance, 12 cores exhibit significantly positive ADR_F, 11 cores show insignificant ADR_F, and one core shows significantly negative ADR_F, thus increasing the percentage of significantly positive ADR_F to 50% (Figure S10). Expanding the spatial scale of microfossil datasets to those with more than one core reduces the number of all datasets to 16 (median $r = 0.16$), among which 50% show a significantly positive ADR_F (Figure S11).

DISCUSSION

Slow sediment accumulation (high time averaging) enhances fossil abundance and diversity. Our results are consistent with the two predictions positing that both abundance and diversity decline with increasing sediment accumulation. Therefore, first, time-averaged fossil abundance is primarily controlled by the lack of dilution by non-skeletal sediment rather than by ecological forcing of standing abundance of living assemblages at yearly (or generational) scales covarying with slow sediment accumulation. This conclusion is supported (1) by the highest abundance of living molluscan assemblages in the Adriatic Sea occurring in the onshore environments subjected to high sediment accumulation, (2) by the total abundance of fossil assemblages exceeding that of living assemblages not affected by time averaging by two orders of magnitude, and by (3) linear mixed-effect models that indicate that the negative effects of sediment accumulation on fossil abundance are not confounded by other factors. Second, the decline in sediment accumulation increases the diversity of fossil assemblages in accordance with the STR. This effect is primarily observed in offshore environments with variable sediment accumulation where fossil diversity exceeds the standing living diversity by a factor of ~2-3.

Positive ADR_F as a signature of temporal scaling. As sediment accumulation reduces both abundance and diversity, and the positive ADR_F disappears when conditioned on sediment accumulation, the variability in abundance and diversity of fossil assemblages is uniquely driven by variability in time averaging. The negative ADR_L also indicates that the ADR_F that is unconditionally positive or positive when conditioned on the energy availability is simply a consequence of variable sediment accumulation that plays a major role in modulating the abundance and diversity of fossil assemblages. The effects of STR on the diversity patterns resulting from variable time averaging of paleontological samples are significant, especially in offshore environments (i.e., deeper than 10 m), and thus cannot be neglected in diversity analyses. When cores systematically differ in sediment accumulation (and thus in time averaging) but within-core variability in sediment accumulation remains relatively low as in this study, the mixed-effect models effectively separate the scaling effects of time averaging on the among-site diversity patterns from the ecological effects of abundance on diversity unrelated to temporal scaling.

Regional ADR_F shaped by onshore-offshore gradients in time averaging. When standing abundances and diversities of communities are negatively related as in our molluscan dataset and time averaging differs between onshore and offshore environments (Figure 5A-B), regional-scale ADR_F patterns can be complex. In two scenarios in Figure 5C, the initial, regional-scale ADR_L is negative in non-averaged assemblages, as observed along the bathymetric gradient in the Adriatic Sea. In the first scenario, assemblages in four environments are equally time-averaged and thus the regional-scale ADR_F can remain negative due to the absence of variability in temporal scaling (i.e., dashed light-gray arrows in in Figure 5C). Such ADR_F can be diagnostic of conditions when the weakly time-averaged fossil record deposited in eutrophic or oxygen-deficient environments exhibit individual-rich but species-poor fossil assemblages dominated by opportunistic species (Filipsson and Nordberg 2004; Tsujimoto et al. 2008). In the second scenario, fossil assemblages in offshore environments, initially with the smallest abundance, are time-averaged to 2000 years, whereas assemblages in onshore environments are time-averaged to two years only, leading to the positive ADR_F (a dashed dark-gray arrow in Figure 5C). The negative ADR_L can thus be reverted into the positive ADR_F when the most productive assemblages are the least time-averaged, as observed in our Adriatic data. This indicates that the positive ADR_F is also determined by the tendency of individual-rich but species-poor assemblages dominated by opportunistic species to occur in environments least prone to time averaging. Despite this additional complexity, the positive ADR_F is still diagnostic of diversity variability controlled by the temporal scaling effect.

Using ADR to extract ecological signals from fossil assemblages. Even in the absence of variability in time averaging, abundance and diversity can be positively associated if they share a common ecological cause such as the total energy availability, leading to both diverse and individual-rich assemblages (Hurlbert 2004; Pautasso et al. 2011; Edgar et al. 2017; Thompson et al. 2020). Therefore, the positive ADR_L can lead to a false positive result with respect to the role of time averaging in modulating diversity. However, several lines of evidence indicate that local-scale ADR_L is typically not positive. First, our analyses of molluscan and foraminiferal assemblages and previous studies (Bolam et al. 2002; Covich et al. 2004; Reiss et al. 2010; Leduc et al. 2012; Schonberg et al. 2014; van der Plas 2019; Dee et al. 2023; Maureaud et al. 2019; Clare et al. 2022) show that the ADR_L at local scales is either negative or close to zero (Figure 6). Second, the ADR_F of molluscan assemblages conditioned on sediment accumulation is not positive. Although both total abundance and biomass are constrained by energy availability that can affect species diversity at local scales, they are also linked by tradeoffs that can lead to a complex ADR (Kadmon and Benjamini 2006, Dornelas 2010). For example, marine benthic communities dominated by small-sized species with high abundance tend to be less diverse than communities dominated by larger but less numerous species (Warwick 1986; Warwick and Clarke 1994). Moreover, species diversity at local scales is not a simple function of local energy availability because species extinction is modulated by population sizes at regional scales of species geographic ranges (attaining few 100s of km or more in marine benthic species). The relationships between diversity and total number of individuals thus tend to be positive only in studies with regional and biogeographic sampling grains (Chase and Ryberg 2004; Storch and Okie 2019; Storch et al. 2018 Craven et al. 2020). The total abundance at local scales is swamped by source-sink factors and tradeoffs between abundances and biomass and thus local ADR_L does not simply scale down from biogeographic ADR_L. The ADR_F that is positive unconditionally or when conditioned on energy availability is thus a useful tool for the detection of scenarios where variability in diversity at local scales is determined by variability in time averaging. Our analyses of macro- and microfossil records suggest that this scaling effect is a common, taxon-independent feature of the fossil record (Fig. 5, Table S4) and thus needs to be considered when assessing paleoecological data.

The effects of temporal scaling can be expected to contribute to fluctuations in local diversity at longer, million-year time scales not only owing to long-term changes in sediment accumulation but also owing to secular changes in mixing and disintegration (Kidwell and

Brenchley 1994). Time averaging documented in the Cenozoic marine fossil record can attain more than 100 kyr (Zimmt et al. 2022), further magnifying the scaling effects because time averaging attaining the scales of species diversification will accelerate species richness accumulation in the logarithmic STR space (Rosenzweig 1998). Although pooling assemblages with variable time averaging into million-year (macroevolutionary) bins with approximately equivalent temporal grain size can alleviate the scaling STR effect, the cost of such a procedure is the loss of spatial and temporal resolution. The stratigraphic records of fossil assemblages with well-resolved age models can use sediment accumulation as a conditioning variable that (1) can remove the biasing effects of differential diversity scaling caused by variable time averaging and (2) can be used in the mixed-effect models to separate the scaling STR effect from the original ADR_L driven by ecological covariance between total abundance and diversity unrelated to scaling. Conditioning ADR on sediment accumulation can thus both identify and correct for the scaling effect induced by time averaging when comparing fossil biodiversity across space and time.

Acknowledgements

We thank three reviewers for detailed and critical comments. This research was supported by the Slovak Research and Development Agency (APVV17-0555, APVV22-0523), Slovak Scientific Grant Agency (VEGA 02/0106/23), and by the Austrian Science Fund (FWF) (grant number P24901).

References

Aller, R.C., 1982. Carbonate dissolution in nearshore terrigenous muds: the role of physical and biological reworking. *Journal of Geology*, 90, 79-95.

Alroy, J. 2010. The shifting balance of diversity among major marine animal groups. *Science*, 329, 1191–1194.

Alroy, J., 2015. The shape of terrestrial abundance distributions. *Science Advances, 1*, e1500082.

Bell, A., and Kelvyn J. 2015. Explaining Fixed Effects: Random Effects Modeling of Time-Series Cross-Sectional and Panel Data. *Political Science Research and Methods* 3: 133–53.

Abbott, S.T., 1997. Mid-cycle condensed shellbeds from mid-Pleistocene cyclothems, New Zealand: implications for sequence architecture. *Sedimentology, 44,* 805-824.

Adler, P.B. and Lauenroth, W.K., 2003. The power of time: spatiotemporal scaling of species diversity. *Ecology Letters*, *6*, 749-756.

Buma, B., Harvey, B.J., Gavin, D.G., Kelly, R., Loboda, T., McNeil, B.E., Marlon, J.R., Meddens, A.J.H., Morris, J.L., Raffa, K.F. and Shuman, B., 2019. The value of linking paleoecological and neoecological perspectives to understand spatially-explicit ecosystem resilience. *Landscape Ecology*, *34*, 17-33.

Balseiro, D. and Waisfeld, B.G., 2014. Evenness and diversity in Upper Cambrian–Lower Ordovician trilobite communities from the Central Andean Basin (Cordillera Oriental, Argentina). *Palaeontology*, *57*, 531-546.

Benito, B.M., Gil-Romera, G. and Birks, H.J.B., 2020. Ecological memory at millennial time-scales: the importance of data constraints, species longevity and niche features. *Ecography*, *43*, 1-10.

Blaauw, M. and Christen, J.A., 2011. Flexible paleoclimate age-depth models using an autoregressive gamma process. *Bayesian Analysis* 6:457-474.

Bolam, S.G., Fernandes, T.F. and Huxham, M., 2002. Diversity, biomass, and ecosystem processes in the marine benthos. *Ecological Monographs*, *72*, 599-615.

Bush, A.M. and Bambach, R.K., 2004. Did alpha diversity increase during the Phanerozoic? Lifting the veils of taphonomic, latitudinal, and environmental biases. *Journal of Geology*, *112*, 625-642.

Carey, S., Ostling, A., Harte, J. and del Moral, R., 2007. Impact of curve construction and community dynamics on the species–time relationship. *Ecology*, *88*, 2145-2153.

46.

Carlucci, J.R. and Westrop, S.R., 2015. Trilobite biofacies and sequence stratigraphy: an example from the Upper Ordovician of Oklahoma. *Lethaia*, *48*, 309-325.

Castillo-Escrivà, A., Mesquita-Joanes, F. and Rueda, J., 2020. Effects of the temporal scale of observation on the analysis of aquatic invertebrate metacommunities. *Frontiers in Ecology and Evolution*, *8*, 561838.

Chao, A., Gotelli, N.J., Hsieh, T.C., Sander, E.L., Ma, K.H., Colwell, R.K. and Ellison, A.M., 2014. Rarefaction and extrapolation with Hill numbers: a framework for sampling and estimation in species diversity studies. *Ecological Monographs, 84*, 45-67.

Chao, A., Kubota, Y., Zelený, D., Chiu, C.H., Li, C.F., Kusumoto, B., Yasuhara, M., Thorn, S., Wei, C.L., Costello, M.J. and Colwell, R.K., 2020. Quantifying sample completeness and comparing diversities among assemblages. *Ecological Research*, *35*, 292-314.

Chase, J.M. and Leibold, M.A., 2002. Spatial scale dictates the productivity–biodiversity relationship. *Nature, 416,* 427-430.

Chase, J.M. and Ryberg, W.A., 2004. Connectivity, scale-dependence, and the productivity–diversity relationship. *Ecology Letters, 7,* 676-683.

Chase, J.M., McGill, B.J., McGlinn, D.J., May, F., Blowes, S.A., Xiao, X., Knight, T.M., Purschke, O. and Gotelli, N.J., 2018. Embracing scale-dependence to achieve a deeper understanding of biodiversity and its change across communities. *Ecology Letters*, *21*, 1737-1751.

Chase, J.M., McGill, B.J., Thompson, P.L., Antão, L.H., Bates, A.E., Blowes, S.A., Dornelas, M., Gonzalez, A., Magurran, A.E., Supp, S.R. and Winter, M., 2019. Species richness change across spatial scales. *Oikos*, *128*, 1079-1091.

Clare, D.S., Culhane, F. and Robinson, L.A., 2022. Secondary production increases with species richness but decreases with species evenness of benthic invertebrates. *Oikos*, e08629.

Coleman, B.D. 1981. On random placement and species-area relations. *Mathematical Biosciences*, *54*, 191-215.

Covich, A.P., Austen, M.C., Bärlocher, F., Chauvet, E., Cardinale, B.J., Biles, C.L., Inchausti, P., Dangles, O., Solan, M., Gessner, M.O. and Statzner, B., 2004. The role of biodiversity in the functioning of freshwater and marine benthic ecosystems. *BioScience*, *54*, 767-775.

Craven, D., van der Sande, M.T., Meyer, C., Gerstner, K., Bennett, J.M., Giling, D.P., Hines, J., Phillips, H.R., May, F., Bannar-Martin, K.H. and Chase, J.M., 2020. A cross-scale assessment of productivity–diversity relationships. *Global Ecology and Biogeography*, *29,* 1940-1955.

Cusson, M. and Bourget, E., 2005. Global patterns of macroinvertebrate production in marine benthic habitats. *Marine Ecology Progress Series*, *297*, 1-14.

Dee, L.E., Ferraro, P.J., Severen, C.N., Kimmel, K.A., Borer, E.T., Byrnes, J.E., Clark, A.T., Hautier, Y., Hector, A., Raynaud, X. and Reich, P.B., Wright A.J., Arnillas C.A., Davies K.F., MacDougall A., Mori A.S., Smith M.D., Adler P.B., Bakker J.D., Brauman K.A., Cowles J., Komatsu K., Knops J.M.H., McCulley R.L, Moore J.L., Morgan J.W., Ohlert T., Power S.A., Sullivan L.L., Stevens C., and Loreau M. 2023. Clarifying the effect of biodiversity on productivity in natural ecosystems with longitudinal data and methods for causal inference. *Nature Communications*, *14*, 2607.

Dornelas, M., 2010. Disturbance and change in biodiversity. *Philosophical Transactions of the Royal Society*, B365, 3719-3727.

Dornelas, M., Chase, J.M., Gotelli, N.J., Magurran, A.E., McGill, B.J., Antão, L.H., Blowes, S.A., Daskalova, G.N., Leung, B., Martins, I.S. and Moyes, F., 2023. Looking back on biodiversity change: lessons for the road ahead. *Philosophical Transactions of the Royal Society B*, *378*, 20220199.

Edgar, G.J., Alexander, T.J., Lefcheck, J.S., Bates, A.E., Kininmonth, S.J., Thomson, R.J., Duffy, J.E., Costello, M.J. and Stuart-Smith, R.D., 2017. Abundance and local-scale processes contribute to multi-phyla gradients in global marine diversity. *Science Advances*, *3*, e1700419.

Egenhoff, S., and Maletz, J. 2007. Graptolites as indicators of maximum flooding surfaces in monotonous deep-water shelf successions. *Palaios*, *22*, 373–383.

Filipsson, H.L. and Nordberg, K., 2004. A 200-year environmental record of a low-oxygen fjord, Sweden, elucidated by benthic foraminifera, sediment characteristics and hydrographic data. *Journal of Foraminiferal Research*, *34*, 277-293.

Finnegan, S., Gehling, J.G. and Droser, M.L., 2019. Unusually variable paleocommunity composition in the oldest metazoan fossil assemblages. *Paleobiology*, *45*, 235-245.

Fridley, J.D., Peet, R.K., Van der Maarel, E. and Willems, J.H., 2006. Integration of local and regional species-area relationships from space-time species accumulation. *American Naturalist*, *168*, 133-143.

Frignani, M. and Langone, L., 1991. Accumulation rates and^{137}Cs distribution in sediments off the Po River delta and the Emilia-Romagna coast (northwestern Adriatic Sea, Italy). *Continental Shelf Research*, *11*, 525-542.

Gallmetzer I., Haselmair A., Stachowitsch M. And Zuschin M. 2016. An innovative piston corer for large-volume sediment samples. Limnology and Oceanography: Methods 14:698–717.

Hsieh, T.C., Ma, K.H. and Chao, A., 2016. iNEXT: an R package for rarefaction and extrapolation of species diversity (H ill numbers). *Methods in Ecology and Evolution*, *7*, 1451-1456.

Hubbell, S.P., 2001. The unified neutral theory of biodiversity and biogeography. In *The Unified Neutral Theory of Biodiversity and Biogeography*. Princeton University Press.

Hurlbert, S.H., 1971. The Nonconcept of Species Diversity: A Critique and Alternative Parameters. Ecology 52:577-586.

Hurlbert, A.H., 2004. Species–energy relationships and habitat complexity in bird communities. *Ecology Letters*, *7*, 714-720.

Kadmon, R. and Benjamini, Y., 2006. Effects of productivity and disturbance on species richness: a neutral model. *American Naturalist*, 167, 939-946.

Kidwell, S.M., 1986. Models for fossil concentrations: paleobiologic implications. *Paleobiology* 12, 6-24.

Kidwell, S.M., 1989. Stratigraphic condensation of marine transgressive records: origin of major shell deposits in the Miocene of Maryland. *Journal of Geology*, *97*, 1-24.

Kidwell, S.M. and Brenchley, P.J., 1994. Patterns in bioclastic accumulation through the Phanerozoic: changes in input or in destruction? *Geology*, *22*, 1139-1143.

Kidwell, S.M., Best, M.M. and Kaufman, D.S., 2005. Taphonomic trade-offs in tropical marine death assemblages: differential time averaging, shell loss, and probable bias in siliciclastic vs. carbonate facies. *Geology*, *33*, 729-732.

Kidwell, S.M., 2013. Time-averaging and fidelity of modern death assemblages: building a taphonomic foundation for conservation palaeobiology. *Palaeontology*, *56*, 487-522.

Labra, F.A., Hernández-Miranda, E. and Quinones, R.A., 2015. Dynamic relationships between body size, species richness, abundance, and energy use in a shallow marine epibenthic faunal community. *Ecology and Evolution*, *5*, 391-408.

Leduc, D., Rowden, A.A., Bowden, D.A., Probert, P.K., Pilditch, C.A. and Nodder, S.D., 2012. Unimodal relationship between biomass and species richness of deep-sea nematodes: implications for the link between productivity and diversity. *Marine Ecology Progress Series*, *454*, 53-64.

Maureaud, A., Hodapp, D., Van Denderen, P.D., Hillebrand, H., Gislason, H., Spaanheden Dencker, T., Beukhof, E. and Lindegren, M., 2019. Biodiversity–ecosystem functioning relationships in fish communities: biomass is related to evenness and the environment, not to species richness. *Proceedings of the Royal Society B*, *286*, 20191189.

McGill, B.J., Hadly, E.A. and Maurer, B.A., 2005. Community inertia of Quaternary small mammal assemblages in North America. *Proceedings of the National Academy of Sciences*, *102*, 16701-16706.

McGlinn, D.J. and Palmer, M.W., 2009. Modeling the sampling effect in the species–time–area relationship. *Ecology*, *90*, 836-846.

McGlinn, D.J., Engel, T., Blowes, S.A., Gotelli, N.J., Knight, T.M., McGill, B.J., Sanders, N.J. and Chase, J.M., 2021. A multiscale framework for disentangling the roles of evenness, density, and aggregation on diversity gradients. *Ecology*, *102*, e03233.

O'Sullivan, J.D., Terry, J.C.D. and Rossberg, A.G., 2021. Intrinsic ecological dynamics drive biodiversity turnover in model metacommunities. *Nature Communications*, *12*, 3627.

Pandolfi, J.M., Staples, T.L. and Kiessling, W., 2020. Increased extinction in the emergence of novel ecological communities. *Science*, *370*, 220-222.

Patrick, C.J., McCluney, K.E., Ruhi, A., Gregory, A., Sabo, J. and Thorp, J.H. 2021. Multi-scale biodiversity drives temporal variability in macrosystems. *Frontiers in Ecology and the Environment*, 19, 47-56.

Pautasso, M., Böhning-Gaese, K., Clergeau, P., Cueto, V.R., Dinetti, M., Fernández-Juricic, E., Kaisanlahti-Jokimäki, M.L., Jokimäki, J., McKinney, M.L., Sodhi, N.S. and Storch, D., 2011. Global macroecology of bird assemblages in urbanized and semi-natural ecosystems. *Global Ecology and Biogeography*, *20*, 426-436.

Pinheiro J, Bates D, R Core Team (2023). nlme: Linear and Nonlinear Mixed Effects Models. R package version 3.1-164, https://CRAN.R-project.org/package=nlme.

Powell, M.G. and Kowalewski, M. 2002. Increase in evenness and sampled alpha diversity through the Phanerozoic: comparison of early Paleozoic and Cenozoic marine fossil assemblages. *Geology*, *30*, 331-334.

Preston, F.W., 1960. Time and space and the variation of species. *Ecology*, *41*, 612-627.

Reiss, H., Degraer, S., Duineveld, G.C., Kröncke, I., Aldridge, J., Craeymeersch, J.A., Eggleton, J.D., Hillewaert, H., Lavaleye, M.S., Moll, A. and Pohlmann, T., 2010. Spatial patterns of infauna, epifauna, and demersal fish communities in the North Sea. *ICES Journal of Marine Science*, *67*, 278-293.

R Core Team (2021). R: A language and environment for statistical computing. R Foundation for Statistical Computing, Vienna, Austria. URL https://www.R-project.org/.

Raia, P., Carotenuto, F., Meloro, C., Piras, P. and Barbera, C. 2011. Species accumulation over space and time in European Plio-Holocene mammals. *Evolutionary Ecology*, 25, 171-188.

Rillo, M.C., Woolley, S. and Hillebrand, H., 2022. Drivers of global pre-industrial patterns of species turnover in planktonic foraminifera. *Ecography*, *2022*, e05892.

Ritter D.N.M., M., Erthal, F., Kosnik, M.A., Kowalewski, M., Coimbra, J.C., Caron, F. and Kaufman, D.S., 2023. Onshore-offshore trends in the temporal resolution of molluscan death assemblages: how age-frequency distributions reveal quaternary sea-level history. *Palaios*, *38*, 148-157.

Rosenzweig, M.L., 1998. Preston's ergodic conjecture: The accumulation of species in space and time. In *Biodiversity dynamics*, 311-348. Columbia University Press.

Scarponi, D. and Kowalewski M. 2007. Sequence stratigraphic anatomy of diversity patterns: Late Quaternary benthic mollusks of the Po Plain, Italy. *Palaios*, *22*, 296-305.

Scarponi, D., Kaufman, D., Amorosi, A. and Kowalewski, M., 2013. Sequence stratigraphy and the resolution of the fossil record. *Geology*, *41*, 239-242.

Scheiner, S.M., Chiarucci, A., Fox, G.A., Helmus, M.R., McGlinn, D.J. and Willig, M.R., 2011. The underpinnings of the relationship of species richness with space and time. *Ecological Monographs*, 81, 195-213.

Schonberg, S.V., Clarke, J.T. and Dunton, K.H., 2014. Distribution, abundance, biomass and diversity of benthic infauna in the Northeast Chukchi Sea, Alaska: Relation to environmental variables and marine mammals. *Deep Sea Research Part II: Topical Studies in Oceanography*, *102*, 144-163.Simonsohn, U., 2018. Two lines: A valid alternative to the invalid testing of U-shaped relationships with quadratic regressions. *Advances in Methods and Practices in Psychological Science, 1*, 538-555.

Smith J., Rillo M.C., Kocsis Á.T., Dornelas M., Fastovich D., Huang H.H.M., Jonkers L., Kiessling W., Li Q., Liow L.H., Margulis-Ohnuma M., Meyers S., Na L., Penny A., Pippenger K., Renaudie J., Saupe E.E., Steinbauer M.J., Sugawara M., Tomašových A., Williams J.J., Yasuhara M., Finnegan S. and Hull P.M. 2023. BioDeepTime: A database of biodiversity time series for modern and fossil assemblages. *Global Ecology and Biogeography, 32,* 1680-1689.

Storch, D., Bohdalková, E. and Okie, J., 2018. The more-individuals hypothesis revisited: the role of community abundance in species richness regulation and the productivity–diversity relationship. *Ecology Letters*, *21*, 920-937.

Storch, D. and Okie, J.G., 2019. The carrying capacity for species richness. *Global Ecology and Biogeography*, *28*, 1519-1532.

Šizling, A.L., Storch, D., Šizlingová, E., Reif, J. and Gaston, K.J., 2009. Species abundance distribution results from a spatial analogy of central limit theorem. *Proceedings of the National Academy of Sciences*, *106*, 6691-6695.

Thompson, P.L., Guzman, L.M., De Meester, L., Horváth, Z., Ptacnik, R., Vanschoenwinkel, B., Viana, D.S. and Chase, J.M., 2020. A process-based metacommunity framework linking local and regional scale community ecology. *Ecology Letters 23*, 1314-1329.

Tomašových, A. and Kidwell, S.M., 2010a. The effects of temporal resolution on species turnover and on testing metacommunity models. *American Naturalist*, *175,* 587-606.

Tomašových, A. and Kidwell, S.M., 2010b. Predicting the effects of increasing temporal scale on species composition, diversity, and rank-abundance distributions. *Paleobiology, 36*, 672-695.

Tomašových, A., Kidwell, S.M. and Barber, R.F., 2016. Inferring skeletal production from time-averaged assemblages: skeletal loss pulls the timing of production pulses towards the modern period. *Paleobiology*, *42*, 54-76.

Tomašových, A., Kidwell, S.M. and Dai, R., 2023. A downcore increase in time averaging is the null expectation from the transit of death assemblages through a mixed layer. *Paleobiology*, 49, 527-562.

Tsujimoto, A., Yasuhara, M., Nomura, R., Yamazaki, H., Sampei, Y., Hirose, K. and Yoshikawa, S., 2008. Development of modern benthic ecosystems in eutrophic coastal oceans: the foraminiferal record over the last 200 years, Osaka Bay, Japan. *Marine Micropaleontology*, *69*, 225-239.

Tumbiolo, M.L. and Downing, J.A., 1994. An empirical model for the prediction of secondary production in marine benthic invertebrate populations. *Marine Ecology Progress Series*, 114, 165-174.

van der Plas, F., 2019. Biodiversity and ecosystem functioning in naturally assembled communities. *Biological Reviews*, *94*, 1220-1245.

van de Pol, M. and Wright, J., 2009. A simple method for distinguishing within-versus between-subject effects using mixed models. *Animal Behaviour*, *77*, 753-758.

Warwick, R., 1986. A new method for detecting pollution effects on marine macrobenthic communities. *Marine Biology*, *92*, 557-562.

Warwick, R.M. and Clarke, K.R., 1994. Relearning the ABC: taxonomic changes and abundance/biomass relationships in disturbed benthic communities. *Marine Biology, 118*, 739-744.

White, E.P., Adler, P.B., Lauenroth, W.K., Gill, R.A., Greenberg, D., Kaufman, D.M., Rassweiler, A., Rusak, J.A., Smith, M.D., Steinbeck, J.R., Waide, R.B. and Yao J. 2006. A comparison of the species–time relationship across ecosystems and taxonomic groups. *Oikos*, *112*, 185-195.

Wittmer, J.M., Dexter, T.A., Scarponi, D., Amorosi, A. and Kowalewski, M., 2014. Quantitative bathymetric models for late Quaternary transgressive-regressive cycles of the Po Plain, Italy. *Journal of Geology*, *122*, 649-670.

Zimmt, J.B., Kidwell, S.M., Lockwood, R. and Thirlwall, M., 2022. Strontium isotope stratigraphy reveals 100 ky-scale condensation, beveling, and internal shingling of transgressive shell beds in the Maryland Miocene. *Palaios*, *37*, 553-573.

Response Predictor	Diversity (saturated model)	Diversity (abundance effect omitted)	Diversity (sediment accumulation effect omitted)	Diversity affected by abundance only /unconditional ADR/	Diversity affected by sedim. accumulation only	Abundance affected by sedim. accumulation and water depth	Abundance affected by sedim. accumulation only	Abundance affected by water depth only
Water depth	0.323	0.32	0.333			0.018		0.031
(inverse of energy avail.)	s.e.=0.020	s.e.=0.020	s.e.=0.020			s.e.=0.019		s.e.=0.021
	p=<0.001	p=<0.001	p=<0.001			p=0.32		p=0.14
Within-core sediment accumulation	0.002	0.003			-0.012	-0.009	-0.01	
	s.e.=0.013	s.e.=0.013			s.e.=0.016	s.e.=0.010	s.e.=0.010	
	p=0.891	p=0.78			p=0.462	p=0.39	p=0.324	
Between-core sediment accumulation	-0.242	-0.276			-0.343	-0.186	-0.193	
	s.e.=0.056	s.e.=0.040			s.e.=0.081	s.e.=0.046	s.e.=0.046	
	p=<0.001	p=<0.001			p=<0.001	p=<0.001	p=<0.001	
Within-core abundance	-0.026		-0.023	-0.019				
	s.e.=0.012		s.e.=0.012	s.e.=0.016				
	p=0.029		p=0.029	p=0.26				
Between-core abundance	0.15		0.73	0.72				
	s.e.=0.184		s.e.=0.15	s.e.=0.31				
	p=0.423		p=<0.001	p=0.028				
AIC	-3244.6	-3242.7	-3234.4	-3094.2	-3095	-3599.1	-3600.2	-3589.4
ΔAIC	0	1.9	12.1	150.4	149.6	1.05	0	9.7
Figure	4G	4G	4C, 4F	4E	3D	4G	3A	4C, 4F

Table 1 – Summary statistics of linear mixed-effect models describing a relationship between sediment accumulation, water depth (inverse of energy availability), fossil diversity and abundance (visualized in figures specified on the bottom of the table). The coefficient (effect size), its standard error and p-values are shown for each predictor. Sediment accumulation and abundance are partitioned into within- and between-core components. The effect of between-core abundance on diversity is unconditionally positive or positive when conditioned on the

water depth but becomes insignificant when conditioned also on between-core sediment accumulation.

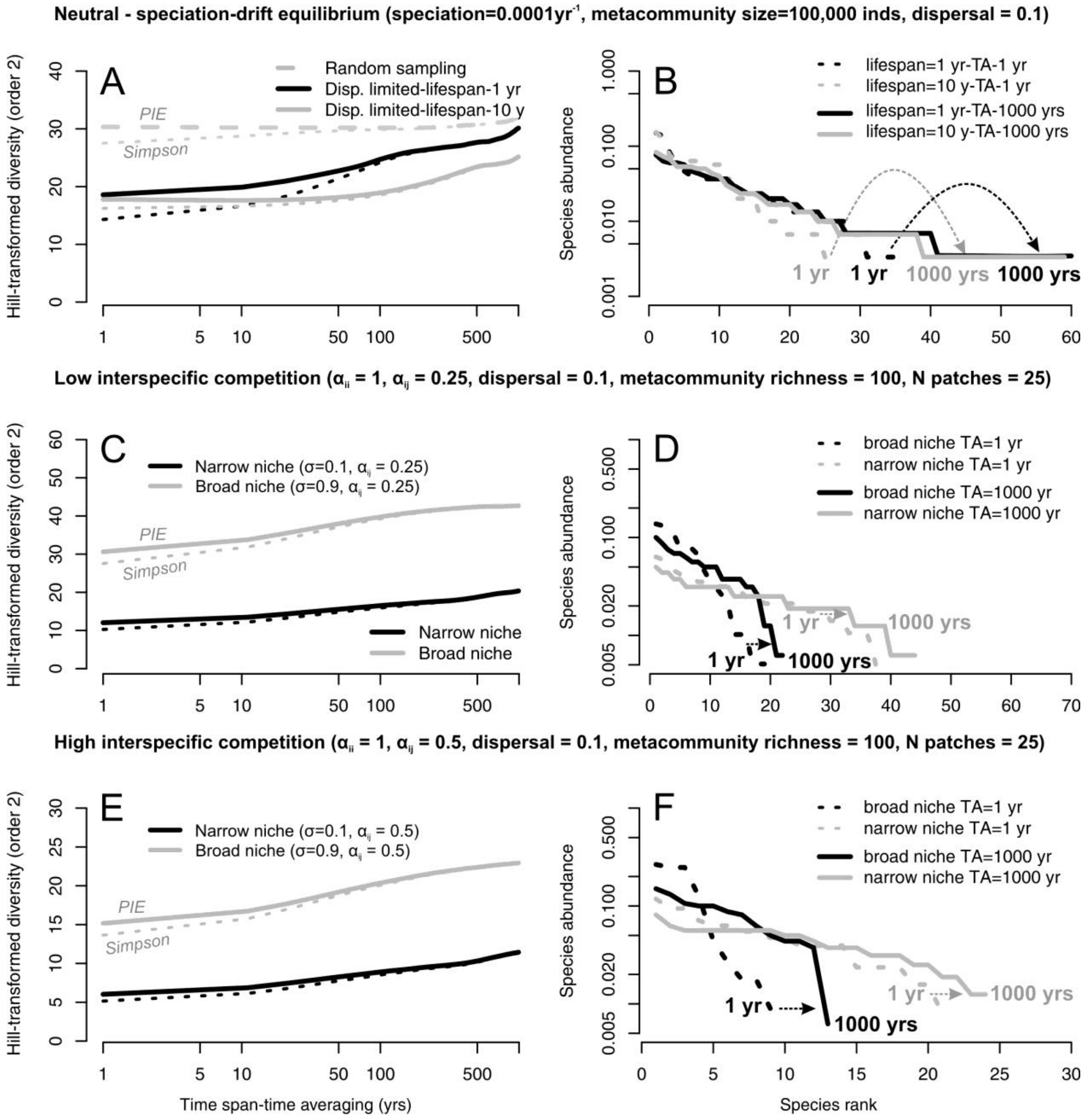

Figure 1. The conceptual figures visualizing the dependency of species diversity on timespan of observation (species-time relationship) that flattens rank-abundance distributions and ultimately leads to positive abundance-diversity relationship. The results are is based on outputs from two standard metacommunity models, including (A-B) neutral, spatially-implicit metacommunity dynamics not limited (dashed gray) and limited by dispersal (solid black and gray) and (C-F) non-neutral, spatially-explicit, dispersal-limited metacommunity dynamics differing in species niche breadths (σ) and in the strength of interspecific competition (α_{ij}). Diversity is defined based on Hill-transformed diversity of order 2, using Simpson diversity (dotted) and PIE-based diversity (solid). The PIE-based diversity remains constant when the neutral dynamic is not limited by dispersal (gray dashed line in A). In this scenario, no

temporal scaling of diversity occurs because when the metacommunity pool is randomly sampled by the local community, the rank-abundance distribution does not change in shape with increasing time averaging. In all other scenarios, both neutral or non-neutral variants, any increase in the PIE-based diversity with increasing time averaging is associated with a decline in the species dominance and in the slope of the rank-abundance distribution as shown in the right column, where time averaging increases from 1 year (solid line) to 1000 years (dashed line). Non-averaged and time-averaged rank abundance distributions in each scenario are rarefied to the same sample size (n = 300 individuals in neutral and 150 individuals in non-neutral models). The speciation timescale is 10,000 years and thus exceeds the maximum time averaging. If time averaging attains speciation timescale, diversity will exponentially increase in logarithmic space. The construction of species-time relationship follows a moving window approach of White et al. (2006). The simulations of neutral model are based on Hubbell (2001) and the simulations of non-neutral models follow Thompson et al. (2020), with R scripts in the Supplement.

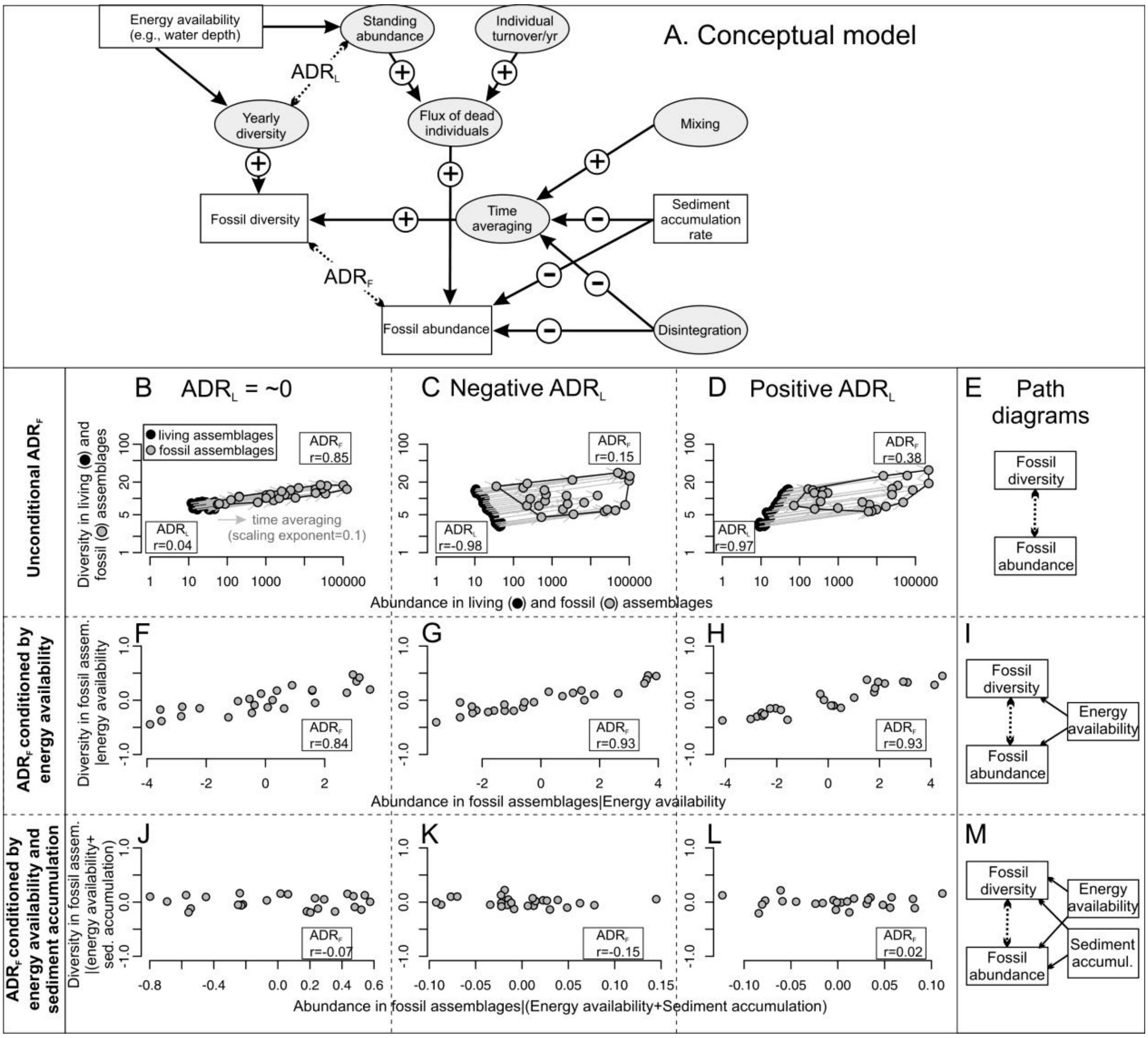

Figure 2. The conceptual path diagram visualizing the variables that affect the abundance-diversity relation in living (ADR$_L$) and in time-averaged fossil assemblages (ADR$_F$) as informed by generalized fossilization models (Tomašových et al. 2023). The nine cartoons and three path diagrams exemplify the combined effect of ADR$_L$ and time averaging on ADR$_F$. (A) The conceptual path diagram. The white boxes represent the variables directly measured or approximated in the fossil record. The gray ellipses visualize the variables not directly measured in our dataset with fossil assemblages. Not all links are specified exhaustively (e.g., sediment accumulation can negatively affect diversity or standing abundance of living assemblage and fossil abundance can positively affect standing abundance via taphonomic feedback). Energy availability can shape both abundance and diversity of living assemblages, and thus determines ADR$_L$. (B-M) Conceptual cartoons visualizing three types of ADR$_L$ patterns (with random, negative and positive ADR$_L$ in three

columns) and three levels of conditioning (with unconditional ADR_F in B-D, ADR_F conditioned on energy availability in F-I, and ADR_F conditioned on energy availability and sediment accumulation in J-M). 25 fossil assemblages are subjected to random time averaging (sampled from a uniform distribution delimited by 3 and 3000 years) and zero disintegration, the STR exponent is 0.1, and gray arrows correspond to the scaling expected under time averaging. Time averaging pulls the ADR of fossil assemblages (gray circles) towards positive values (upper row), although the sign of the unconditional ADR_F depends on the initial configuration of living assemblages (black circles). When the ADR_L is ~0 (B), the unconditional ADR_F will be positive owing to the scaling effect. When the ADR_L is negative (C), the unconditional ADR_F will be less negative, but the scaling effect is cancelled out by the negative sign of the ADR_L. When the ADR_L is positive (D), the unconditional ADR_F will remain positive, regardless of the scaling effect. The positive effect of time averaging on abundance and diversity emerges in all scenarios when the ADR_F is conditioned on the ecological variable (e.g., energy availability) that forces the negative or positive ADR_L (F-H). Such positive ADR_F disappears when conditioned on the energy availability *and* sediment accumulation (J-L), providing a key insight into the contribution of time averaging to variability in fossil abundance and diversity. The path diagrams corresponding to each row are shown in the right column.

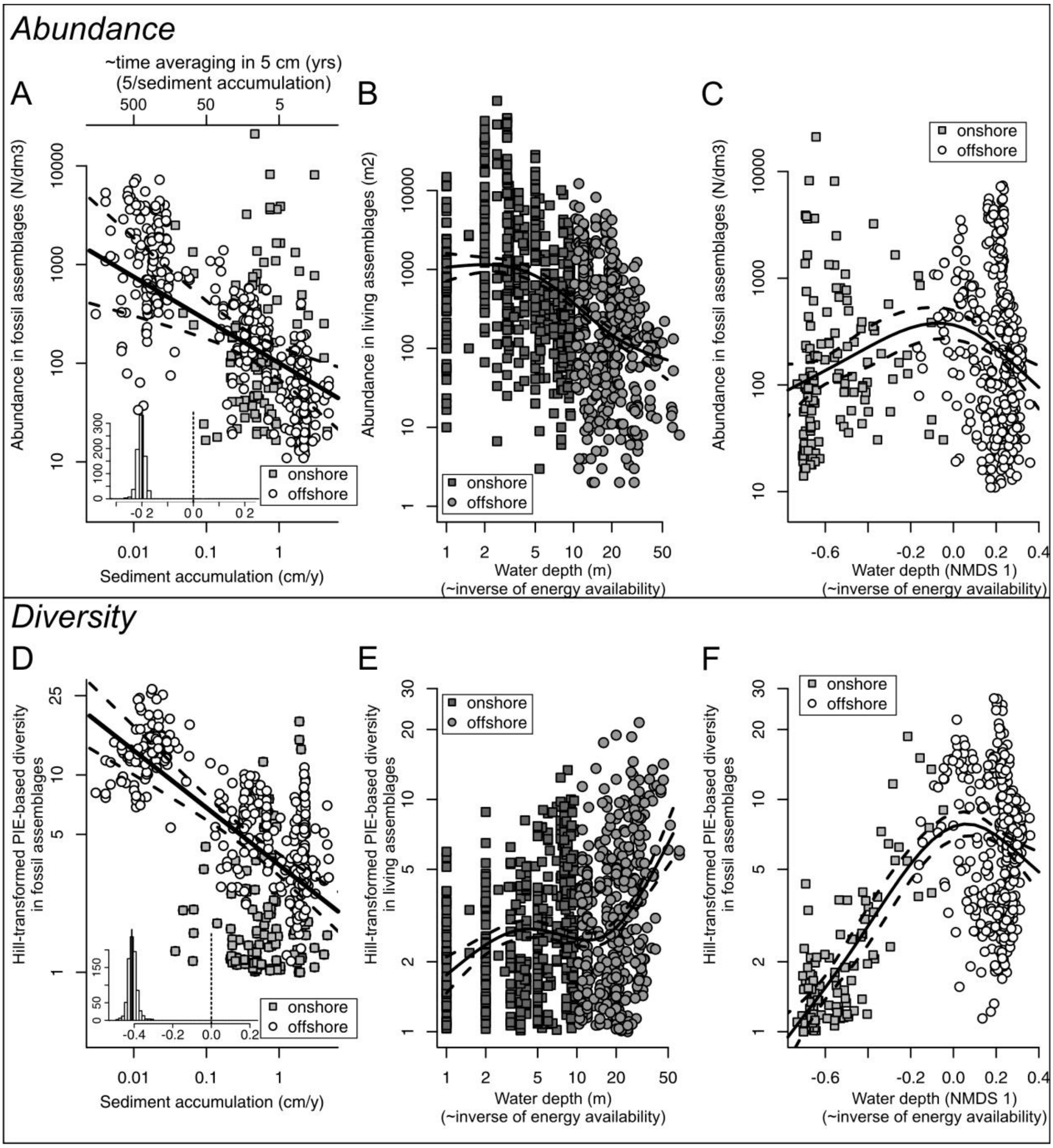

Figure 3. Sediment accumulation covaries negatively both with the abundance and diversity of fossil assemblages as predicted by the scaling effects of time averaging on both variables (via the species-time relationship). Sediment accumulation affects negatively both abundance (A) and PIE-based diversity (D) in fossil assemblages (time averaging on the top axis corresponds to the inverse of sediment accumulation, neglecting the thickness of the mixed layer). Abundance declines with water depth (B), whereas the PIE-based diversity increases with water depth (E) in living (non-averaged) assemblages. Abundance does not covary with water depth (C), and the PIE-based diversity increases with water depth in time-averaged fossil assemblages (F). Abundance~accumulation and diversity~accumulation relations in A

and D are estimated with the linear mixed-effect models (Table 1). The bathymetric gradients in abundance and diversity in living and fossil assemblages in B-C and E-F are fitted with generalized additive models (with 95% confidence intervals). The insets with frequency distributions capture negative effects of the effects of sediment accumulation on abundance (A) and diversity (D), based on the resampling of posterior estimates of sediment accumulation from Bayesian age-depth models. Note: N/dm^3 – number of individuals in fossil assemblages per sediment volume. Source data: Table S1-S2.

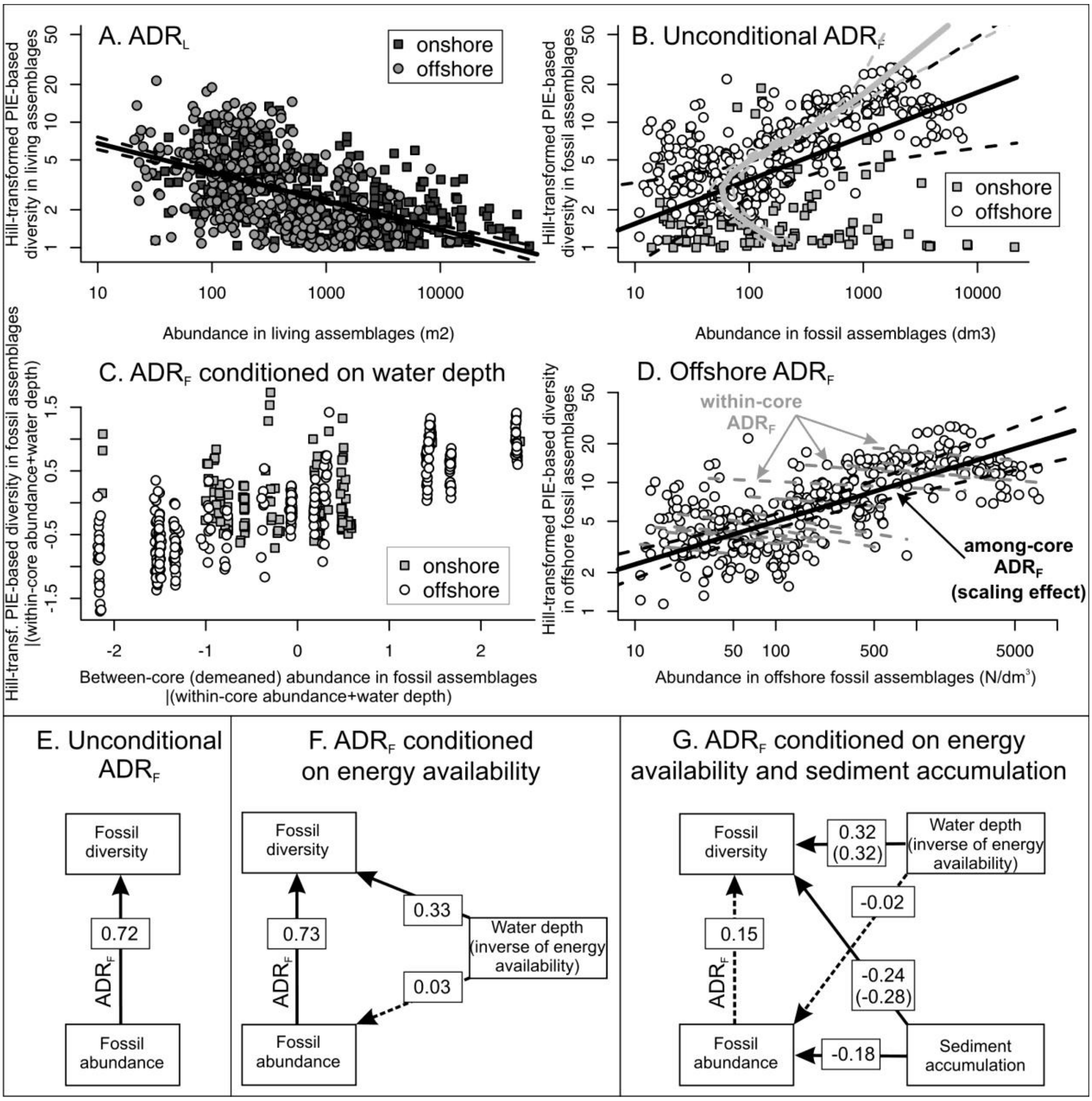

Figure 4. ADR is pulled towards the positive values as living assemblages are transformed into fossil assemblages as predicted by the hypotheses postulating the effects of time averaging (via sediment accumulation) on fossil abundance and diversity, and becomes insignificant when conditioned on sediment accumulation. Raw (unconditional) ADR is negative in living assemblages (A) and positive in fossil assemblages (B), and ADR$_F$ remains positive when conditioned on the water depth (C-D). The black lines represent the fit by the generalized least-square model (with spherical correlation structure) in the ADR$_L$ (A) and by the linear mixed-effect model (cores as random effects and temporal autocorrelation modelled by the autoregressive process of order 1) in the ADR$_F$ (B). The gray lines in B correspond to the U-shaped fit to the ADR$_F$ by the generalized additive model. This ADR$_F$ pattern

represents a trace of the scaling pathway that pulled offshore assemblages (with low diversity and low abundances) towards high fossil abundance and diversity. (C) Positive ADR_F conditioned on the water depth, with residuals of between-core abundance effect on the x axis and diversity residuals on the y axis. (D) Focusing just on offshore assemblages allows for plotting the actual abundances and diversities rather than their residuals. The linear mixed-effect model with random slopes and intercepts visualizes that within-core ADR_F tends to be negative whereas the between-core effect of abundance on diversity is markedly positive. (E-G) Path diagrams visualizing the positive relation between fossil abundance and diversity (unconditional ADR_F, E), the ADR_F remains positive when conditioned on the water depth (F), and the ADR_F disappears when conditioned on the water depth and sediment accumulation (G) on the basis of 489 fossil assemblages in the Adriatic Sea. The numbers in white boxes represent standardized regression coefficients from linear mixed-effect models (with abundance and sediment accumulation effects corresponding to the between-core effects in Table 1), the dashed links reflect insignificant paths. The numbers in parentheses in G refer to the model where the effect of abundance on diversity is set to zero. Source data: Table S1-S2.

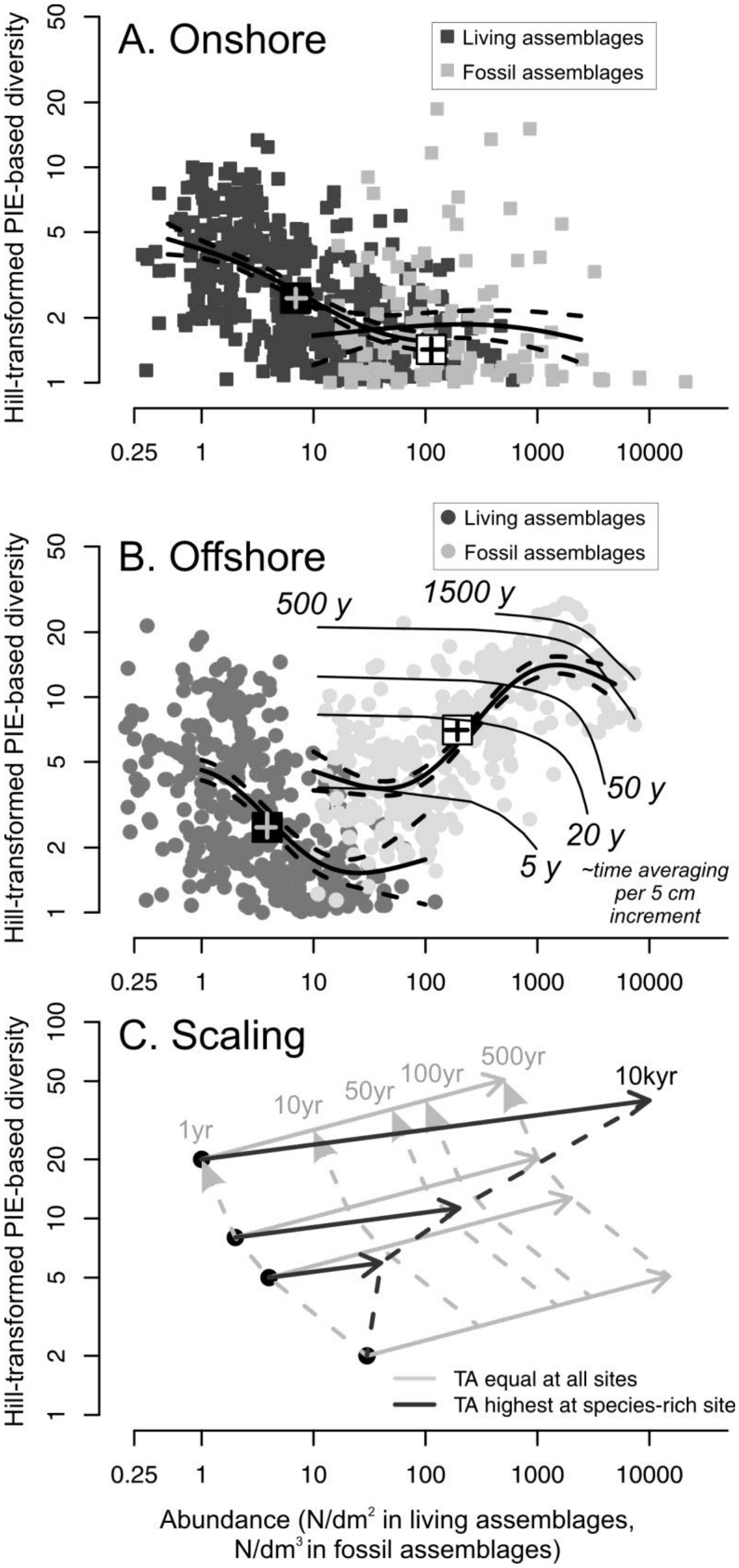

Figure 5. Reconstructing the scaling pathway leading from the negative ADR_L to the positive ADR_F by embedding living and fossil assemblages in the same abundance-diversity space. The small differences in abundance and diversity between living (black) and fossil

assemblages (gray) in onshore environments with high sediment accumulation (>0.1 cm/y) and thus very low time averaging (A) contrast with the ladder-like progression of abundance and diversity in offshore environments (B), where sediment accumulation is lower than 0.1 cm/y and more variable, leading to the positive ADR_F. The contours correspond to approximate time averaging (in years) in 5 cm-increments (the inverse of sediment accumulation in years/cm multiplied by 5), fitted by generalized additive models. The boxes show mean abundance and diversity values with 95% bootstrapped confidence intervals. (C) The abundance shift along the x-axis depends on the sediment accumulation, assuming no disintegration and the diversity shift along the y-axis depends on the scaling slope of the species-time relationship (here, STR exponent is equal to 0.15, and all molluscs are assumed to have temporally-constant abundance and 1-year lifespan). The initial *local-scale* ADR_L is negative in non-averaged assemblages (four black circles, with poorly-diverse assemblages with high abundance and highly-diverse assemblages with low abundance). The shift towards the positive (regional-scale) ADR_F is magnified when species-rich but individual-poor assemblages are more averaged (to 10 kyr) than species-poor and individual-rich assemblages, as observed in the northern Adriatic Sea (black arrows with STR exponent = 0.1, with endpoints connected by the dashed black line). In the absence of variability in time averaging, the ADR_F will remain negative (dashed gray lines). In A and B, as the volume of fossil samples varies between ~0.8-1.3 dm^3, we standardize densities in living assemblages to N/dm^2 in these order-of-magnitude analyses (Van Veen grabs used for sampling living assemblages penetrate to sediment depths of 5-15 cm and are thus similar to the thickness of core increments ranging between 4-10 cm). Source data: Table S1-S2.

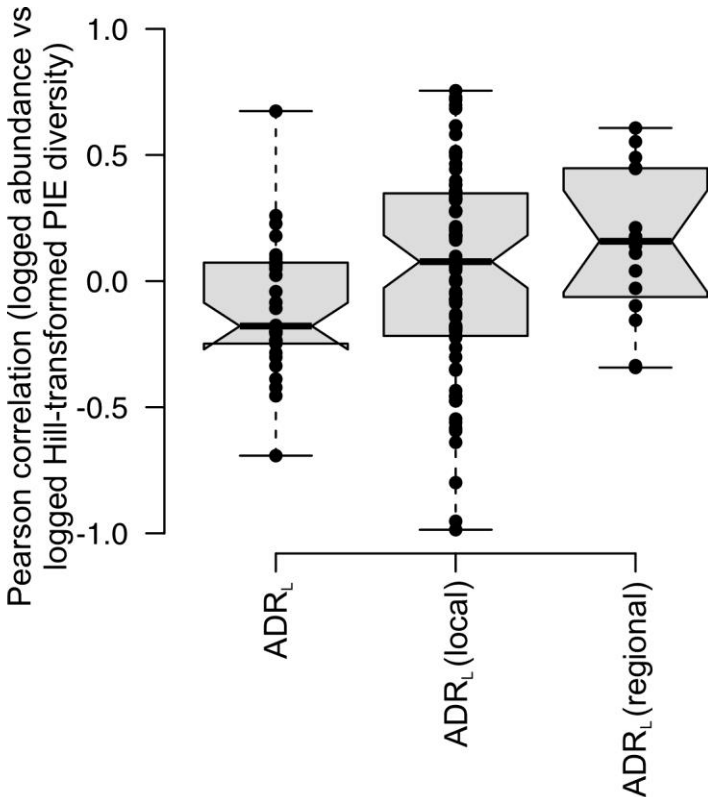

Figure 6. The systematic difference in the sign of the ADR$_L$ and ADR$_F$ exhibited by benthic foraminifers can reflect the effect of variable time averaging, with 29% of local FDRs and 50% of regional FDRs exhibiting significantly positive relation. The ADR$_L$ patterns estimated on the basis of spatial surveys (n=30) are on average slightly negative. The ADR$_F$ patterns are based on fossil assemblages observed in local stratigraphic series (n=73) and in regional spatio-temporal datasets with at least two cores (n=25). Data sources: Table S3 and S4.

Supporting Information for

Abundance-diversity relationship as a unique signature of temporal scaling

Adam Tomašových*, Michał Kowalewski, Rafał Nawrot, Daniele Scarponi, Martin Zuschin

*Corresponding author: Adam Tomašových

Email: geoltoma@savba.sk

This PDF file includes:

- Supporting text
- Figures S1 to S11
- Tables S1 to S5
- SI references
- Data files and scripts:
  https://datadryad.org/stash/share/dEfyOr0s3aBnuN3KMAIoeI-mi1eZ_Eg--fxyjIzzsXM

Supporting text

Sampling. The dataset with 1,150 living assemblages compiled from 27 studies (Figure S1, Table S1) is restricted to assemblages with a minimum size of 10 individuals. In some cases, it includes repeated bi-annual or annual sampling (such assemblages were not pooled to avoid analytical time averaging). The assessment of the abundance-diversity relationship is based on assemblages that were completely censused at the species level. Several surveys focused on estimating the abundance of the most common species (*Lentidium mediterraneum* or *Chamelea gallina*) in the shallowest habitats document extremely high population densities, exceeding 20,000-30,000 individuals/m^2. Although they do not capture the sample total abundance (i.e., all molluscan individuals), we use these densities as minimum estimates of abundance in assessments of the depth-abundance relationship in Figure 3. Such incomplete samples that lack data on abundances of other species were excluded from other analyses of ADRs.

The 26 cores with 489 fossil assemblages span from siliciclastic deltaic settings with a high sediment accumulation rate (in the NW Adriatic Sea and in the Gulf of Trieste) to current-winnowed and sediment-starved, siliciclastic-carbonate settings with a low sediment accumulation rate (in the NE segment). The cores archive the recentmost centuries at sites with a high sediment accumulation rate (0.2-2 cm/y) or span ~9-10 kyr (corresponding to the flooding of the northern Adriatic shelf) at sites with low sediment accumulation rates (<0.02 cm/y). These short cores were split into 4-5 cm-thick increments; assemblages from all increments were surveyed. Fifteen cores (> 10 m-long) from the Po coastal plain (deposited at ~ 1 cm/y during the highstand phase and at < 0.25 cm/y during the transgressive phase, Scarponi et al. 2013) were split into 5 and 10 cm increments that were sampled either at regular intervals separated by 1-3 m or more densely at intervals characterized by facies shifts. 489 fossil assemblages cover delta front (n=105), barrier island (n=32), transgressive sand sheet (n=68), prodelta (n=207), and offshore transition facies associations (n=78). Total abundance refers to the total number of uniquely identifiable specimens (with umbo or hinge preserved) and thus is not affected by differences in fragmentation among sites or increments. When sample sizes exceeded more than several thousands of individuals, increments were split into fractions and the fraction-level count was multiplied by the fraction inverse to derive the total abundance per total increment volume (e.g. if half of the sample was processed, the total number of individuals was multiplied by two) (Gallmetzer et al. 2019).

Age models and sediment accumulation rates. Short and densely-sampled cores include M13, M14, M20 and M21 in the proximal parts of the Po prodelta, POS514-GC-25-5 in the distal parts of the Po prodelta, M28 and M29 in the Isonzo prodelta (Bay of Panzano), M38 in the current-winnowed Gulf of Venice, M1 and M53 at Piran, and M44 at Brijuni. Fifteen (> 10 m-long) cores from the Po coastal plain include 240-S8, 205-S4, 205-S14, 205-S10, 205-S9, 205-S7, 204-S7, 205-S1, 205-S2, 256-S3, 205-S6, 204-EM-S5, 188-EM-S4, 187-EM-S12, and 187-C Goro. Sediment cores were sampled with two sampling strategies that partly differ in core length, core diameter and density of increment sampling. Age models were directly estimated for cores Po 3-M13, Po 4-M21, Panzano-M28, Piran-M53, and extrapolated to spatially-proximate cores Po 3-M14, Po 4-M20, Panzano-M29, and Piran-M1 with highly – similar lithological attributes and stratification patterns (Figure S3). In contrast to shorter piston and gravity cores, age models at the coastal Po Plain are based on a smaller number of age-dating levels (at least two dated levels per systems tract) (Figure S2). The core lithology and fossil molluscan assemblages in these cores were described previously (Scarponi and Kowalewski 2004, 2007; Kowalewski et al. 2015; Gallmetzer et al. 2017, 2019; Tomašových et al. 2018; Berensmeier et al. 2023).

The primary references for 26 cores are as follows: 240-S8 (Campo et al., 2020; Cheli et al., 2021), 205-S4 (Scarponi et al. 2013; Amorosi et al., 2017; 2020; 2021), 205-S14 (Scarponi et al., 2013; Amorosi et al., 2017), 205-S10 (Sarti et al., 2009; Campo et al., 2020), 205-S9 (Sarti et al., 2009; Bruno et al., 2017; Amorosi et al., 2020), 205-S7 (Cibin et al., 2005; Scarponi et al., 2013; Amorosi et al., 2017), 204-S7 (Calabrese et al., 2009; Amorosi et al., 2017; Bruno et al., 2019), 205-S1 (Amorosi et al., 2003; Sarti et al., 2009), 205-S2 (Campo et al., 2020; Amorosi et al., 2021), 256-S3 (Severi et al., 2005; Campo et al., 2020), 205-S6 (Sarti et al., 2009; Amorosi et al., 2017, 2020), 204-EM-S5 (Amorosi et al., 2017), 204-EM-S4 (Amorosi et al., 2017), 188-EM-S5 (Amorosi et al., 2017), 187-EM-S12 (Amorosi et al., 2017), 187-C_Goro_I (Sarti et al., 2009), Po 3 M13, Po 3 M14, Po 4 M20, Po 4 M21 (Tomašových et al. 2018), Panzano M28 and M29 (Tomašových et al. 2017), Piran 1 M1 and Piran 2 M53 (Mautner et al. 2018, Tomašových et al. 2019), Venice M38 (Gallmetzer et al. 2019), Brijuni M44 (Schnedl et al. 2018, Tomašových et al. 2022), and Poseidon core

POS514 – GC-25-5 (Berensmeier et al. 2023). The top-core age estimation of cores drilled at the Po Plain, which was a swampy area until a few decades or centuries ago, is based either on the year of final land reclamation of the area where the core was drilled (the cores 205-S1, 205-S2; 204 EM-S5, and 188 EM-S5 were drilled in areas that were reclaimed in 1964 AD, the core 205-S6 was drilled in area reclaimed in 1919 AD, the core 205-S7 in area reclaimed in 1933 AD, and the core 205-S10 in area reclaimed in 1958 AD) or on the basis of information in geological maps and seismic profiles (Scarponi et al. 2013).

Bayesian age-depth models and sediment accumulation (cm/y) were estimated with the Bacon function (rbacon package, Blaauw and Christen 2011, Blaauw et al. 2021) on the basis of 1) single-shell radiocarbon estimates (with the mean age and age error represented by standard deviation based on the radiocarbon calibration), 2) amino-acid and radiocarbon estimates from multiple shells dated from the same core increment (with the mean of age distribution and its standard error; the spread of within-increment ages directly reflects natural time averaging of co-occurring shells as the measurement error is typically smaller than range of ages induced by slow sedimentation and high mixing in these cores, Scarponi et al. 2013; Tomašových et al. 2017, 2018, 2022), and 3) the timing of the boundary between the highstand systems tract and the maximum flooding zone constrained on the basis of seismic stratigraphy (~7,000 years BP, Amorosi et al. 2017). The calibration of amino acid and radiocarbon ages and among-core correlations are presented in the references cited in the previous paragraph, the input data for the Bacon function are listed in the Supplementary Table 6. The parameter of the prior beta distribution for autocorrelation among sediment accumulation rates within cores was set to a minimum dependency (mean=0.01) with shape = 100 (corresponding to a small variance in memory). The prior beta distribution for sediment accumulation time (in years/cm) was set to the overall long-term sedimentation time (core duration/core thickness) and the shape parameter of the beta distribution was set to 0.5 (when core spanned several systems tracts) or 2 (when empirical age data do not indicate any major change in sediment accumulation rate).

Sediment accumulation rates based on age models in these cores are moderate to high (0.1-5 cm/y) in facies associations deposited in intertidal and upper shoreface environments. They are more variable in lower shoreface to offshore environments, ranging from very low (~0.001 cm/y) at locations affected by winnowing and sediment starvation to high (~5 cm/y) at deltaic settings (Figure S4-S5). This bathymetric decline in sediment accumulation is in accord with modern, decadal-scale estimates in deltaic settings and with the bathymetric decline in sediment accumulation observed in the northern Adriatic Sea (Frignani and Langone 1991).

The effect of sediment accumulation on abundance and diversity or conditional independence between them may be assessed only when age models are based on a sufficiently high number of dated intervals. When based on a few dated intervals, the estimates of sediment accumulation rate will not resolve smaller-scale variability in sedimentation (and thus in time averaging) when interpolating sediment accumulation rates to undated levels. The estimates of sediment accumulation may be decoupled from time averaging, thus potentially also not tracking the true variability in time averaging, but Holocene fossil assemblages in the Adriatic Sea tend to show the close relation between residence times of molluscan remains in 5-10 cm-thick increments predicted on the basis of sediment accumulation and direct estimates of time averaging based on dating of at least ten shells per increment (Scarponi and Kowalewski 2013, Tomašových et al. 2022).

All analyses are performed with R Core Team (2021), version 4.3.0, including the following packages: nlme (Pinheiro et al. 2023), mgcv (Wood 2011, vegan (Oksanen et al. 2020), datawizard (Patil et al. 2020), AICcmodavg (Mazerolle et al. 2023), truncnorm (Mesmann et al. 2018), iNEXT (Hsieh et al. 2016), piecewiseSEM (Lefcheck 2016), synchrony (Gouhier T.C. and Guichard 2014), dplyr (Wickham 2016), ggplot2 (Wickham 2016), and rbacon (Blaauw and Christen 2011).

The species-time relationship (STR). The estimates of diversity that are independent of sample size, such as the PIE-based diversity or rarefied species richness, will not increase with increasing time averaging when assemblages are randomly assembled (not limited by dispersal) from metacommunities with temporally constant species-abundance distributions (gray dashed line in Figures 1A). This scenario is also directly equivalent to the random sampling model when an increase in species richness reflects increasing sampling from a static species pool (Coleman 1981).Therefore, except in rare scenarios where the temporal dynamic of assemblages is not limited by dispersal and local assemblages are random samples from the metacommunity that follows a random-walk dynamic (drift-diversification, Hubbell 2001), diversity estimates based on sample size standardization do not correct for among-sample differences in time averaging. When the duration of the time series approaches the time scale of species diversification, PIE-based diversity will increase with increasing time averaging even under a random metacommunity assembly.

Once time averaging integrates across community assembly limited by dispersal or driven by non-neutral dynamic, different values of time averaging will produce misleading differences in diversity. We note that the scaling effect does not necessarily increase the evenness measures that have species richness in the denominator because the sensitivity of these indices to time averaging depends on the ratio of higher-order diversity relative to species richness. For example, in the absence of immigration from other regions and/or when turnover in species identity at the local scale is minor, species richness will increase with time, averaging less than the diversity of order two, thus also increasing evenness. When species richness increases with time averaging at a higher rate than the diversity of order two owing to significant turnover in species identity (as can happen in neutral models), evenness can decline with increasing time averaging.

Bathymetric gradients in diversity and abundance. We assess differences in abundance and diversity between living and fossil assemblages within habitats by partitioning living assemblages (shallower and deeper than 10 m) and fossil assemblages (defined by two main groups of samples in the cluster analyses that correspond to the assemblages dominated by *Lentidium* and *Chamelea* on the one hand and by species preferring offshore habitats on the other hand) into two equivalent depth segments differing not only in exposure to salinity fluctuations, in hydrodynamic conditions and grain size but also in community composition. The Bray-Curtis and Hellinger distances generate equivalent clusters and NMDS ordination patterns (Figure S6-S8). The shallower (onshore) assemblages are dominated by *Lentidium* and *Chamelea* (inhabiting nearshore environments), and the deeper (offshore) assemblages by *Varicorbula, Turritellinella, Timoclea* and *Gouldia* (thriving in offshore transition and offshore environments). This categorization allows us to assess whether the abundance and diversity of fossil assemblages exceed those of living assemblages, as predicted by the R-sediment model (Kidwell 1986), and to approximate how the ADR_F is shaped by time averaging while controlling for differences related to bathymetry. The analyses based on the relationship between the Hill-transformed sample size-corrected Shannon diversity (Chao et al. 2014), fossil abundance, and sediment accumulation generate almost identical results. In our datasets, the PIE-based diversity also correlates strongly with Pielou's J in living (r = 0.85, p<0.0001) and fossil assemblages (r =0.91, p<0.0001).

As the positive FADR patterns are predicted to be observed when fossil assemblages form under different sediment accumulation, we primarily focus on the regional-scale ADR (observed in assemblages collected in multiple sediment cores that capture larger bathymetric and geographic gradients or cover longer temporal extents than individual sediment cores) in our analyses of fossil assemblages in the northern Adriatic Sea, although we also report the local-scale ADR_F (observed in individual sediment cores). The mean abundance of living assemblages declines from 4,730 at depths < 5 m to 853 at 10-20 m and to 243 at depths > 20 m. Fossil assemblages preserved in offshore environments are on average equally rich in individuals as those from onshore environments, with mean abundance equal to 650-750 individuals/dm^3 on both sides of the ordination gradient. The mean PIE-based diversity increases with depth both in living assemblages (r = 0.22, p < 0.0001) by a factor of ~2-3, from 3.1 at depths < 10 m to 3.2 at 10-20 m and 4.6 at depths > 20 m and in fossil assemblages (r = 0.68, p = <0.0001). The PIE-based diversity of fossil assemblages increases by a factor of ~3 when comparing onshore and offshore environments (from 2.7 in assemblages with negative scores to 8.4 in assemblages with positive scores), parallel with declining sediment accumulation. However, the diversity of fossil assemblages in offshore environments is variable, ranging from almost monospecific assemblages up to highly diverse assemblages with > 20 equally abundant species. The bathymetric decline in the dominance structure in fossil assemblages parallels the increase in evenness (r [Pielou's J] = 0.7, p < 0.0001). The Hill-transformed Shannon diversity gives similar results as PIE-based diversity. The correlation between sediment accumulation and PIE-based diversity is negative when the effect of abundance is factored out. The diversity of individual-rich fossil assemblages (with more than 250 individuals/dm^3) is bimodally-distributed, whereas the diversity of individual-poor fossil assemblages (<250 individuals/dm^3) is distributed uniformly or unimodally.

Structural equation models. In parallel with the linear mixed-effect models, we also use structural equation models (SEM, Schumacker and Lomax 2010) to assess whether a decline in sediment accumulation increases the abundance and diversity of fossil assemblages and at the same time accounts for the positive effects of abundance on diversity if conditioned by sediment accumulation. Although this simple approach does not incorporate temporal autocorrelation and heterogeneity among cores, the among-variable relationships directly parallel the setup of linear mixed-effect models. The saturated model (df=0) is compared with a reduced model without any unique effect of abundance on diversity on the basis of the Akaike information criterion and on the basis of the likelihood-ratio Chi-square statistic. The full model visualized in Figure 2B (AIC = 4182.9) explains 48% of the variation in fossil abundance by variability in sediment accumulation and water depth and 74% of the variation in diversity by variability in sediment accumulation, water depth, and fossil abundance. All paths are significant at $p < 0.05$, except for the effect of depth on abundance ($p = 0.2$) and abundance on diversity ($p = 0.18$). 74% of the variation in diversity is also explained by variability in sediment accumulation and water depth in the model where the covariance between fossil abundance and fossil diversity is set to zero (AIC = 4183.2, likelihood-ratio test $\chi^2 = 1.77$, $p=0.18$). The unconditional positive covariance between the abundance and diversity of fossil assemblages is thus entirely accounted for by the effect of the sediment accumulation.

Abundance-diversity relation in molluscan fossil assemblages. The frequency and the strength of the ADR_F in the stratigraphic record depends on the LADR (Figure 2A-C), on disintegration and mixing processes, on variability in time averaging, and on the magnitude of the slope of the STR, and is thus difficult to predict. The raw ADR_F exhibiting the U-shaped pattern reflects the complex interaction between the negative ADR_L and the time averaging effect pulling the abundance-diversity relation towards positive values (Figure 4B). When the ADR_L is not random and rather negative, as in the northern Adriatic Sea, conditioning the ADR_F on the main variable that covaries with the ADR_L (water depth) leads to a strongly positive relationship (Figure 4C-D). We note that in a scenario where the scaling exponent of the STR increases with depth but time averaging is equally high at all depths, offshore assemblages will be more diverse than onshore assemblages but not more rich in individuals. Therefore, the bathymetric shift in the STR slope alone, not associated with variability in time averaging, is not sufficient to generate the abundance-diversity relation.

In any case, the positive ADR_F can primarily emerge when abundance and diversity patterns are assessed in stratigraphic successions deposited under variable sediment accumulation. ADR_F patterns within individual cores in our Adriatic dataset are rarely significantly positive because most are characterized by a limited variability in sediment accumulation and fossil abundance. Simple Pearson correlations observed within individual cores are highly variable, ranging between -0.7 and 0.63 (with significantly positive value observed in one core only). 13 out of 20 cores exhibit a range of time averaging values among 5-10 cm increments that are smaller than 50 years, approximated on the basis of the inverse of sediment accumulation. The strongly positive ADR_F emerges in regional-scale analysis only when assemblages within cores are time-averaged to varying degrees. Similarly, although the microfossil records show the positive ADR_F also at the scale of individual cores, the proportion of datasets with significantly positive ADR_F patterns increases to 50% when assessed at regional scales spanning multiple cores.

Microfaunal records. Our criteria used in the selection of time series with fossil assemblages from the Marben subset of the Biodeeptime database include explicit information on volume- or mass-standardized estimates of per-assemblage total abundance, complete species-level census abundance counts not excluding any rare species, at least ten samples with quantitative abundance data per time series, and the associated age model. We assessed the frequency of the significantly positive ADR_F patterns at the scale of individual cores (73 datasets) and at the scale of larger regions that consist of at least two cores (25 datasets). These datasets span five orders of magnitude in duration, from 10 years to more than 100,000 years. However, we also assessed the frequency of cores with a significantly positive ADR_F relative to the total number of cores in settings where the preconditions for a significantly positive ADR_F are met. For this purpose, we exclude the cores with low variability in time averaging and abundance in a subset of analyses focused on individual sediment cores. We use these three criteria to select this subset of cores - coefficients of variation in time averaging and in fossil abundance across the cores exceed 0.25 (i.e., time averaging and fossil abundance vary by more than 25% relative to the mean abundance) and mean sediment accumulation rates are not high (with mean sediment accumulation smaller than 0.2 cm/y). When computing the coefficient of variation in time averaging between all adjacent assemblages in each core or region, we use an inverse of the sediment accumulation as a proxy for time averaging (ignoring the depth of the mixed layer). The generalized least-square models that account for temporal autocorrelation (with the same structure as in the mixed-effect models) return a similar frequency of significantly positive ADR_F patterns for individual time series.

Effects of disintegration and false negatives. The increase in fossil abundance driven by the lack of dilution can be counteracted by the disintegration of skeletal remains. Disintegration can reduce the abundance of dead individuals accumulating in the surface mixed layer to below the standing abundance of their source living assemblage (Kidwell 2002). Post-mortem age-frequency distributions indicate that the disintegration of molluscan remains occurs on decadal scales in the northern Adriatic Sea (Tomašových et al., 2022). Therefore, fossil abundances observed in this setting are expected to be smaller relative to scenarios where disintegration is slower or can be neglected. However, the fossil abundance in the core samples (mean = 730 N/dm^2, max = 7,400 N/dm^2) exceeds the living abundance observed in benthic surveys (mean = 6 N/dm^2, max = 122 N/dm^2) by more than two orders of magnitude in offshore environments. Therefore, the effect of disintegration does not cancel out the negative relation between fossil abundance and sediment accumulation. In onshore environments, the mean fossil abundance (mean = 650 N/dm^2, max = 21,000 N/dm^2) exceeds the mean living abundance (mean = 50 N/dm^2, max = 1,370 N/dm^2) by a smaller factor than in offshore environments, probably reflecting the effect of higher dilution of molluscan remains by clastic sediments.

In general, the positive ADR_F can be a conservative criterion of the temporal scaling effect owing to the potential for false negatives. Even when fossil remains disintegrate rapidly, stochastic mixing by burrowers can still allow some remains to be buried into the historical layers and thus will be incorporated into the stratigraphic record. This dynamic can lead to highly time-averaged but shell-poor assemblages (Tomašových et al. 2023), leading to no differences in fossil abundance between weakly-averaged assemblages with lower diversity and highly time-averaged assemblages with higher diversity. The scenario where time averaging does not covary with fossil abundance can thus generate false negative results concerning the role of time averaging even when diversity differences among fossil assemblages are triggered by differences in time averaging.

Role of anthropogenic impacts. Both abundance and diversity of living assemblages collected in the late 20th and in the 21st century can be negatively affected by anthropogenic impacts, thus magnifying the differences between non-averaged living assemblages and time-averaged fossil assemblages or artificially contributing to the positive ADR_F (e.g., when some weakly time-averaged assemblages have low diversity because they were sourced by impacted communities over the past decades). First, excluding the Anthropocene samples (typically represented by assemblages sourced by communities in the 20th century and located in the upper 20 cm of sediment cores, exceptionally in the upper 90 cm at Po Delta) also generates a significantly positive ADR_F in the whole northern Adriatic Sea ($r = 0.46$, $p < 0.0001$) and also within offshore environments ($r = 0.71$, $p < 0.0001$). Second, the disparity in abundance between fossil and living assemblages driven by time averaging can be biased up because abundances of some molluscan species and the overall molluscan production have been depressed over the last century owing to anthropogenic eutrophication, hypoxia, trawling, or pollution relative to the earlier Holocene conditions (Haselmair et al. 2021). However, the 20th-century decline in molluscan population densities is probably not sufficient to generate the order-of-magnitude increase in abundance in time-averaged fossil assemblages relative to their living counterparts.

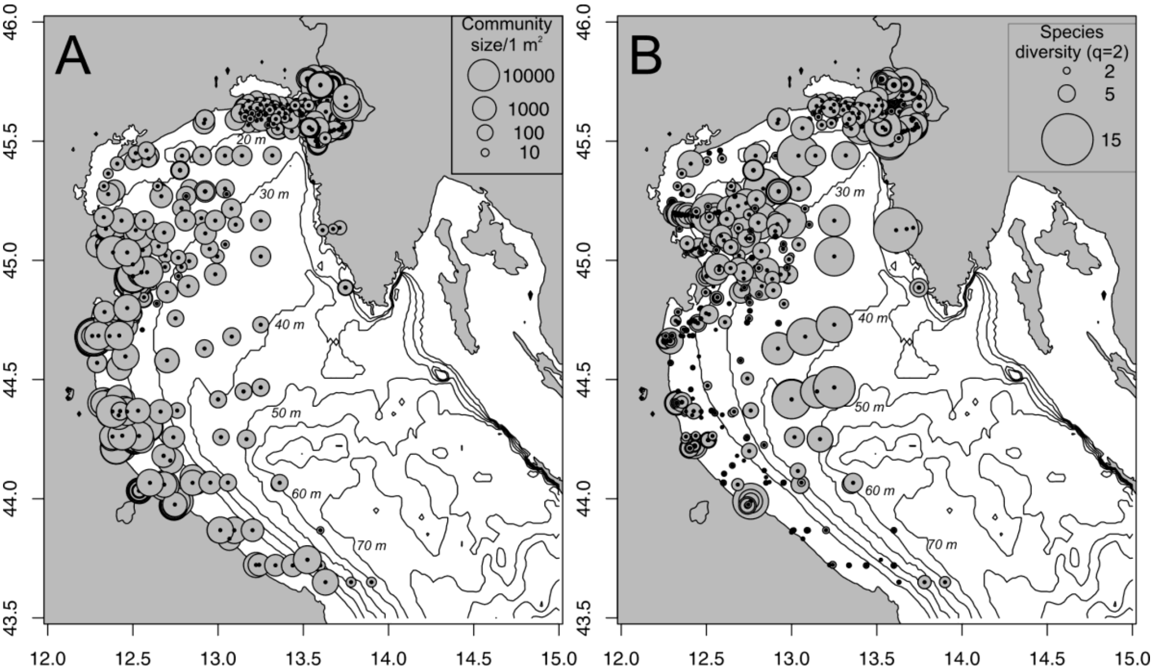

Figure S1. Geographic distribution of living molluscan assemblages analyzed in this study visualizes the negative relation between the standing abundance of molluscs and their diversity in the northern Adriatic Sea. A. Total molluscan abundance in living assemblages (individuals/m2) tends to decline with increasing water depth. B. The Hill-transformed PIE-based diversity of living assemblages tends to increase with increasing water depth. Data sources for assemblages collected alive: Ambrogi and Ambrogi 1985, Ambrogi et al. 1995, ARPAE 2010-2019, Chiantore et al. 2001, ENEA database, Forni et al. 2005, Haselmair et al. 2021, ISPRA 2012, Mavric et al. 2010, Moodley et al. 1998, Nasi et al. 2020, N'Siala et al. 2008, Occhipinti-Ambrogi et al. 2002, Orel et al. 1987, Poluzzi et al. 1981, Prevedelli et al. 2001, Rigotti 2019, Scardi et al. 2000, Seneš 1989, Simonini et al. 2005, Solis-Weiss et al. 2001, Targusi 2011, Tomašových et al. 2019, Weber and Zuschin 2013, Zavodnik and Vidakovic 1987, Zucchi Stolfa 1979.

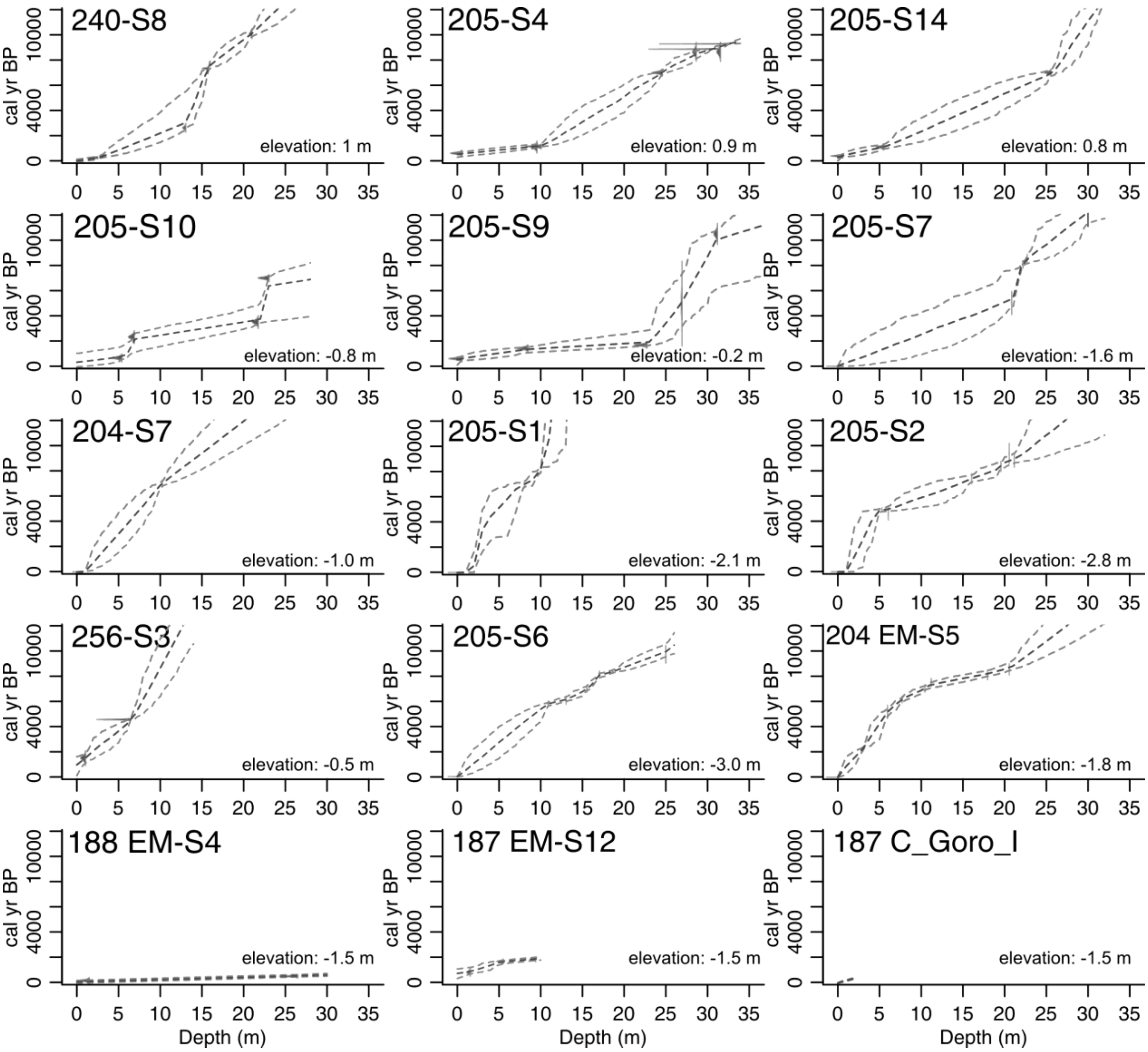

Figure S2. Age models for the Po Plain cores. Age model sources: 240-S8 (Campo et al., 2020; Cheli et al., 2021 [sample CE]), 205-S4 (Scarponi et al. 2013; Amorosi et al., 2017; 2020; 2021), 205-S14 (Scarponi et al., 2013; Amorosi et al., 2017), 205-S10 (Sarti et al., 2009; Campo et al., 2020), 205-S9 (Sarti et al., 2009; Bruno et al., 2017; Amorosi et al., 2020), 205-S7 (Cibin et al., 2005; Scarponi et al., 2013; Amorosi et al., 2017), 204-S7 (Calabrese et al., 2009; Amorosi et al., 2017; Bruno et al., 2019), 205-S1 (Amorosi et al., 2003; Sarti et al., 2009), 205-S2 (Campo et al., 2020; Amorosi et al., 2021), 256-S3 (Severi et al., 2005; Campo et al., 2020), 205-S6 (Sarti et al., 2009; Amorosi et al., 2017, 2020), 204-EM-S5 (Amorosi et al., 2017), 204-EM-S4 (Amorosi et al., 2017), 188-EM-S5 (Amorosi et al., 2017), 187-EM-S12 (Amorosi et al., 2017), 187-C_Goro_I (Sarti et al., 2009).

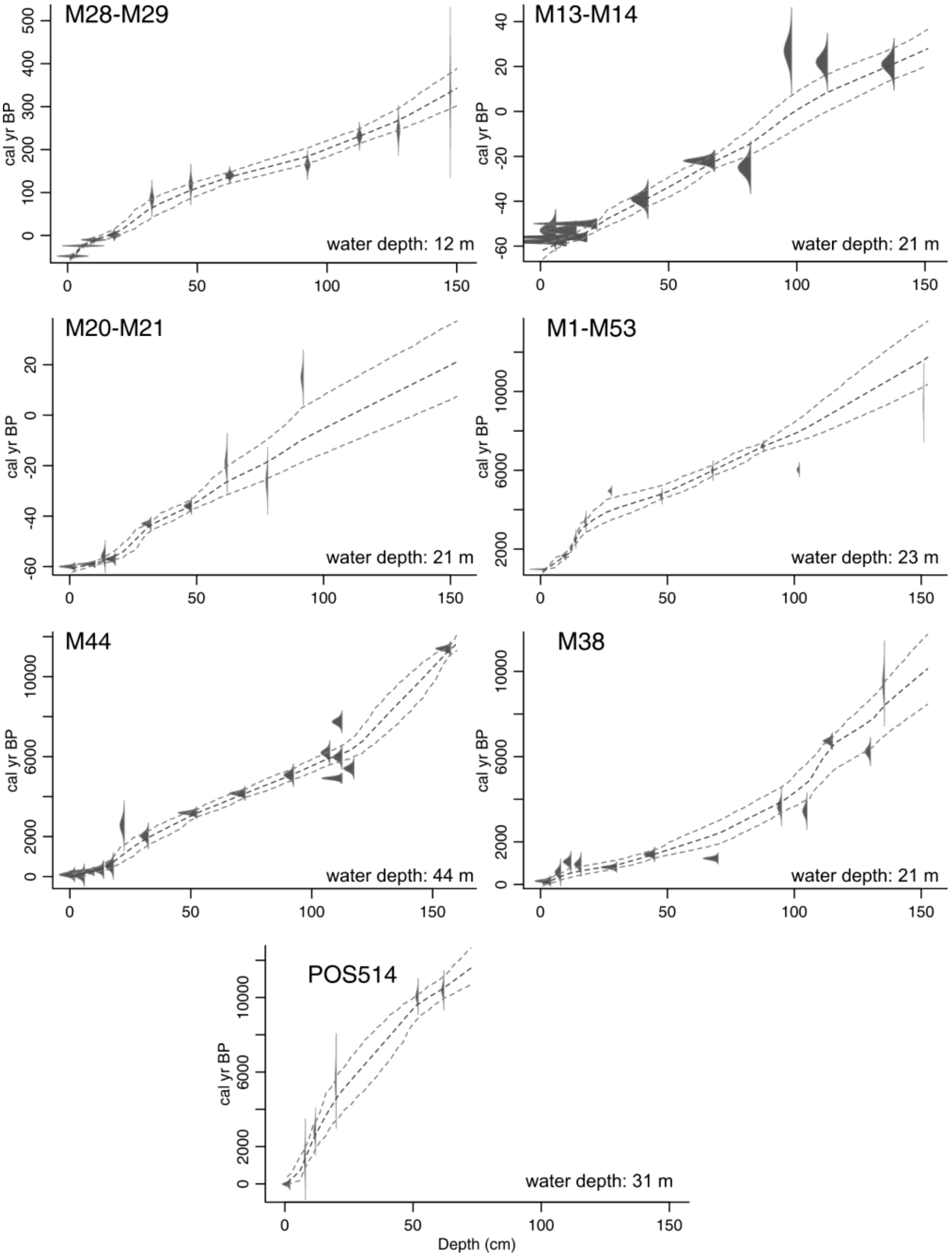

Figure S3. Age models for the 1.5 m-long cores, with boxplots representing frequency distributions of geochronological ages (i.e., postmortem ages) of molluscan remains based on amino acid racemization calibrated by ^{14}C. The age models are partly informed by age distributions but also by additional sedimentological and geochronological data (210Pb and ^{14}C of plant remains). Sources for age distributions and age models: Po 3 M13 and Po 4 M21 (Tomašových et al. 2018), Panzano M28 (Tomašových et al. 2018), Piran 1 M1 and Piran 2 M53 (Mautner et al. 2018, Tomašových et al. 2019), Venice M38 (Gallmetzer et al. 2019), Brijuni M44 (Schnedl et al. 2018, Tomašových et al. 2022), and Poseidon core POS514 – GC-25-5 (Berensmeier et al. 2023).

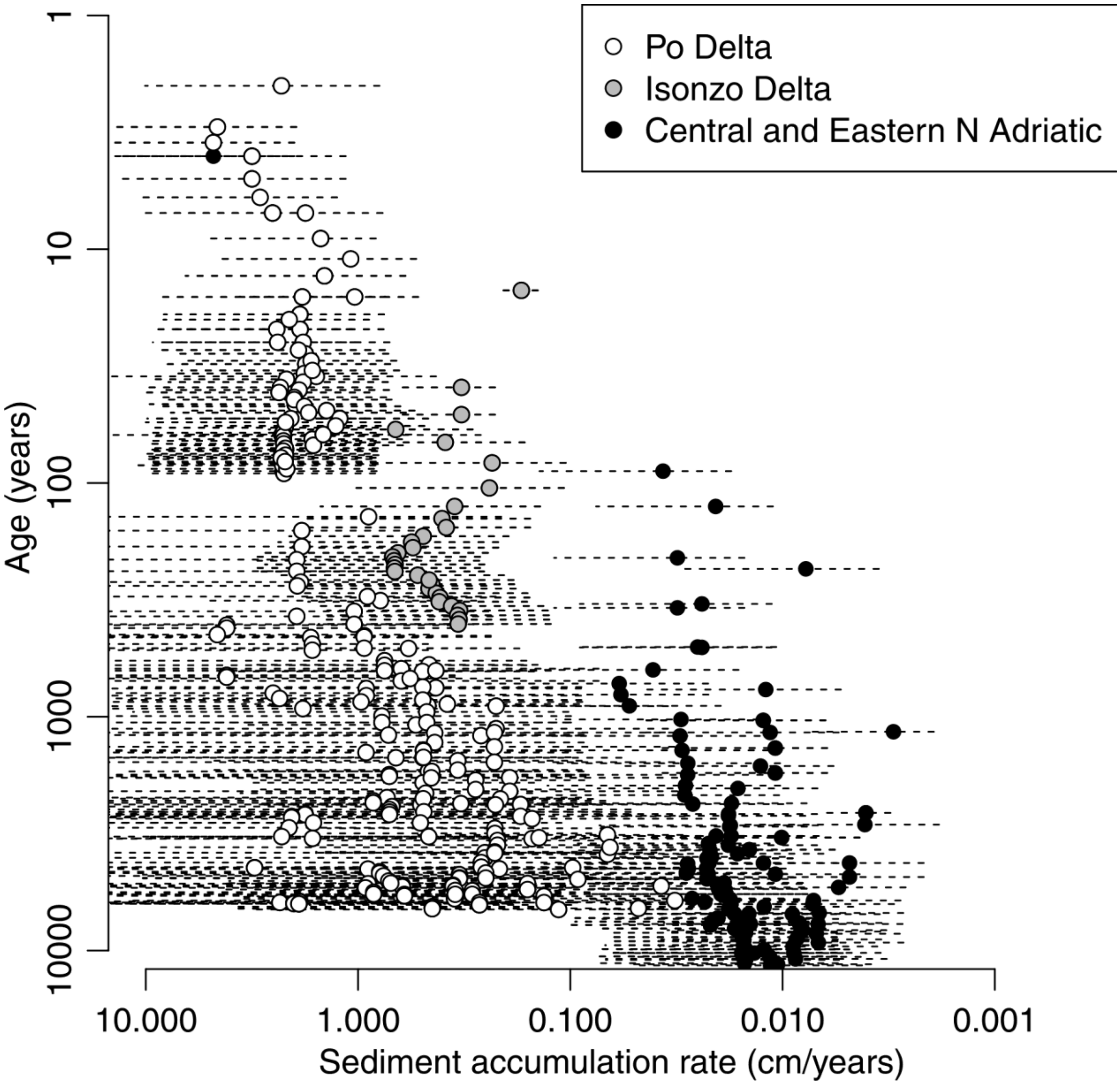

Figure S4. The distribution of sediment accumulation rates with respect to assemblage age. Variability in sediment accumulation rates is given by the extent of error bars corresponding to the interquartile range bracketed by the 25th and 75th percentiles (based on the posterior distribution of sediment accumulation rates).

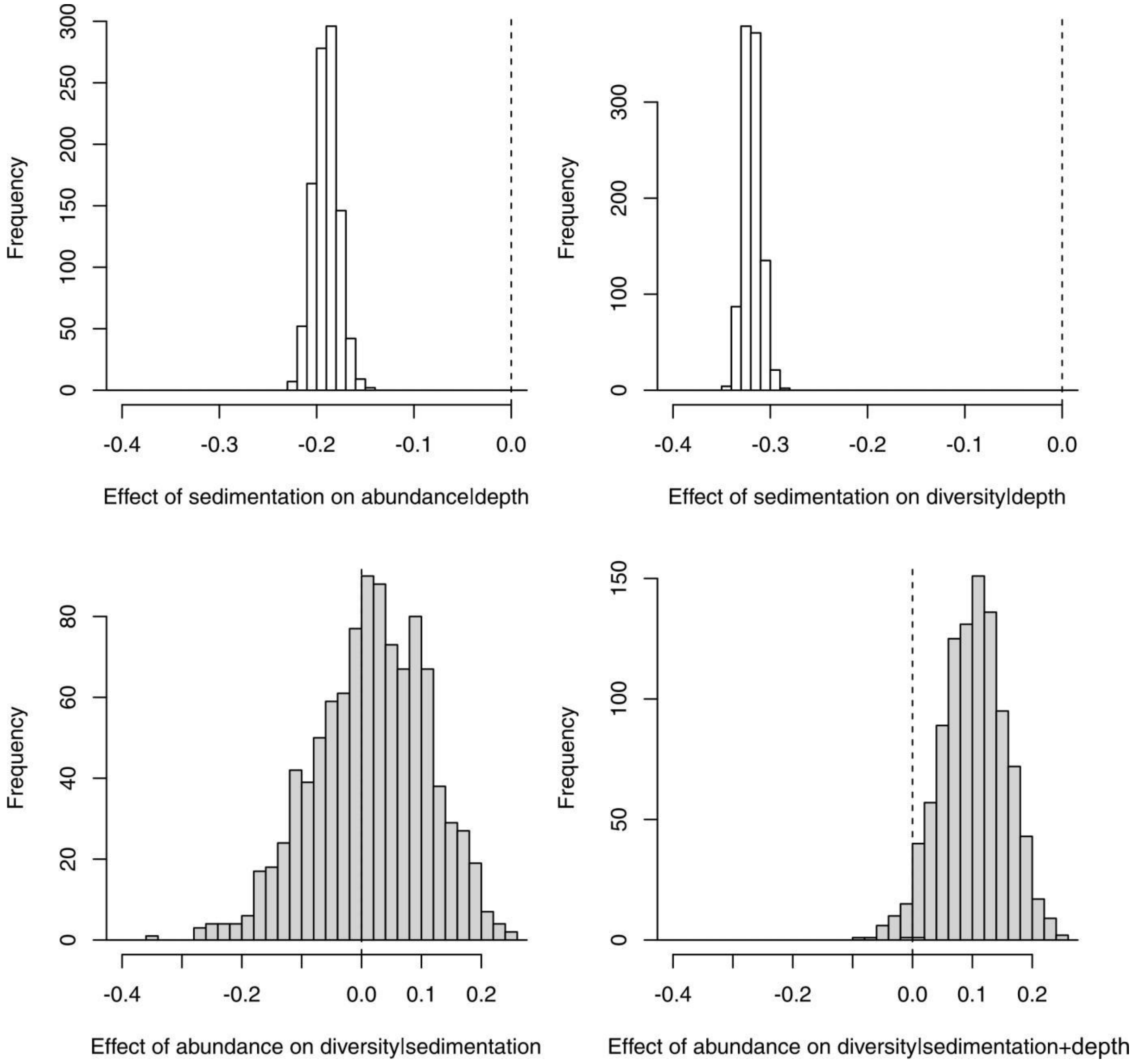

Figure S5. The frequency distributions of the fixed effects (effects of sedimentation on abundance and diversity in the upper row and the effect of abundance on diversity conditioned by sedimentation or by both sedimentation and water depth in the bottom row) expected under the repeated sampling of sediment accumulation rates from posterior distributions derived from Bayesian age-depth models. They show that the effects of sediment accumulation are consistently negative and the abundance effect on diversity conditioned by sediment accumulation does not differ from zero.

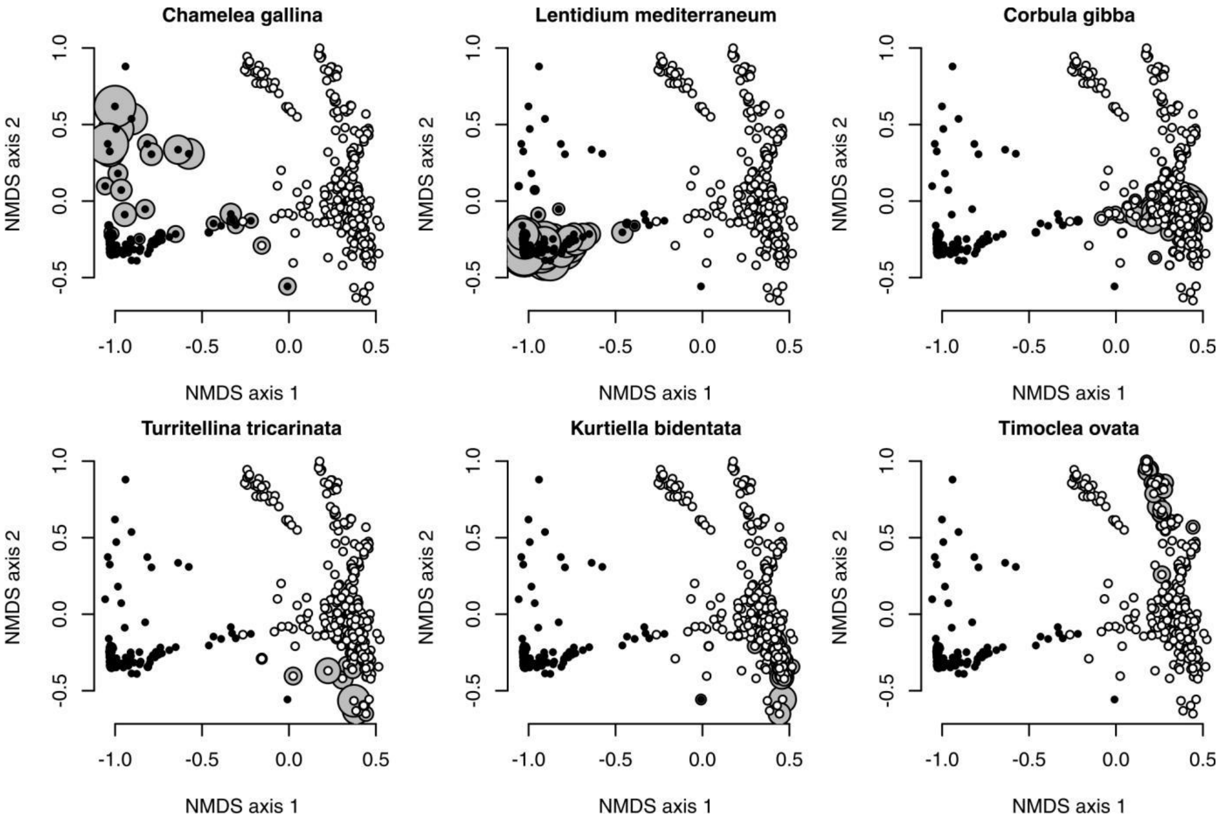

Figure S6. NMDS orders fossil molluscan assemblages along a bathymetric gradient, with onshore assemblages possessing negative NMDS axis 1 scores (black circles) and offshore transition and offshore assemblages possessing positive NMDS axis 1 scores (white circles). NMDS is based on proportional abundances and Chord distance. The categorization of assemblages into onshore and offshore groups follows the clusters in Figure S8. The sizes of gray circles are scaled according to the proportional abundances of individual species.

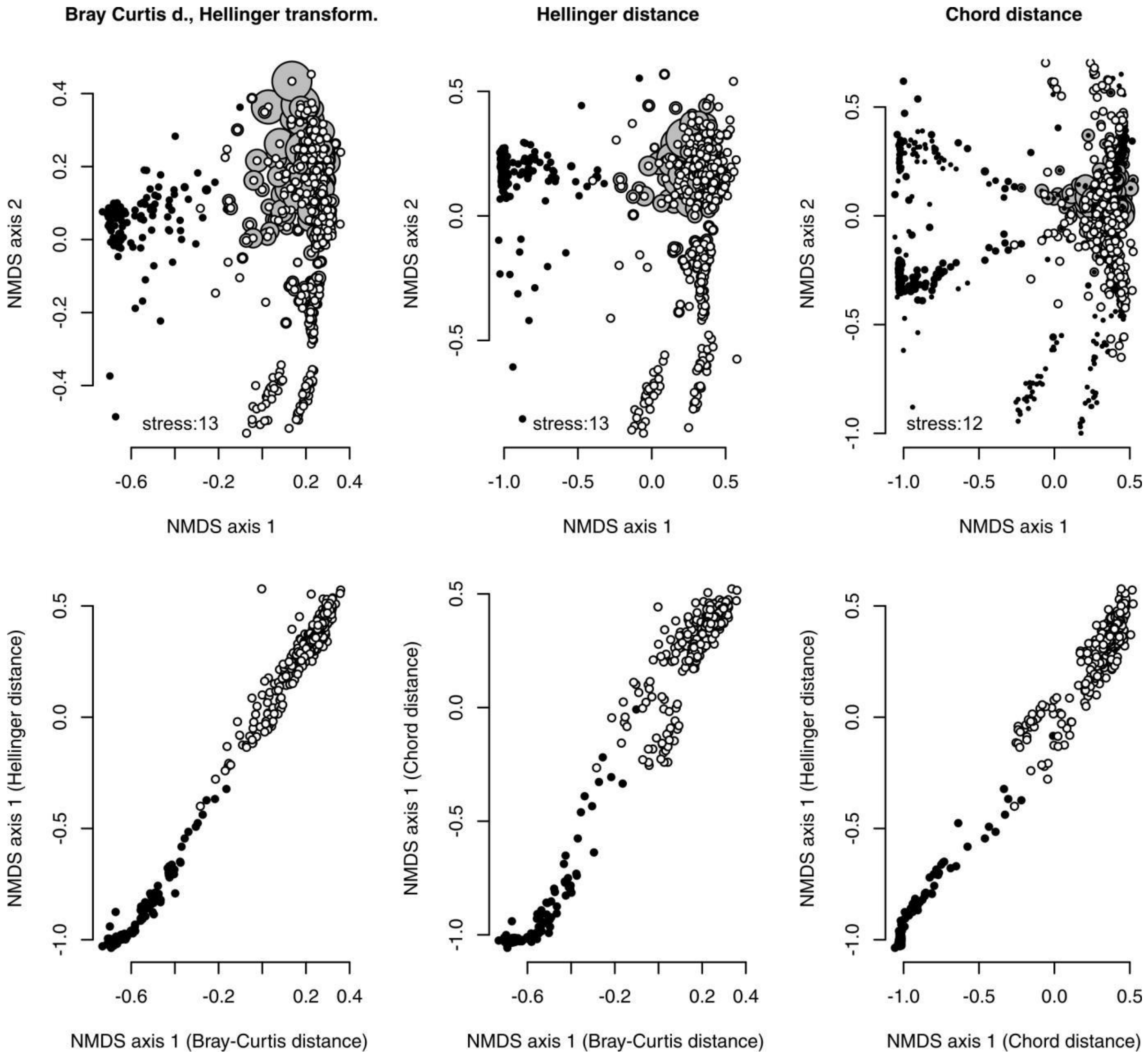

Figure S7. Sensitivity of ordinations to the underlying dissimilarity metric. The first NMDS axis is an indicator of water depth the ordering of assemblages is highly similar on the basis of Bray-Curtis, Hellinger and Chord distances. Onshore assemblages are represented by black circles and offshore assemblages by white circles. The categorization of assemblages into these two groups follows the clusters in Figure S8.

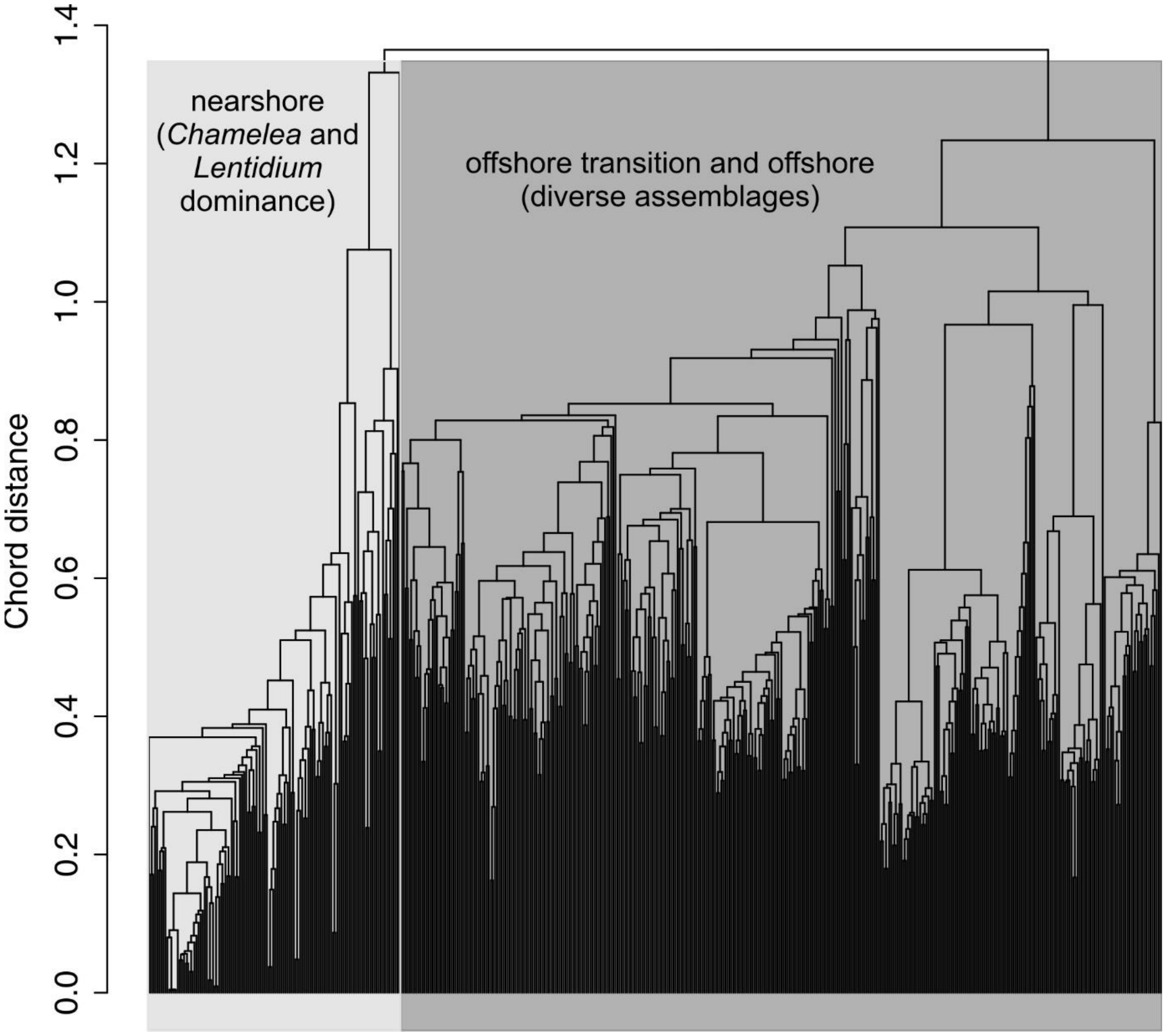

Figure S8 – Cluster analysis based on average linking method and Chord distance, separating two main groups of assemblages, corresponding to two main environments.

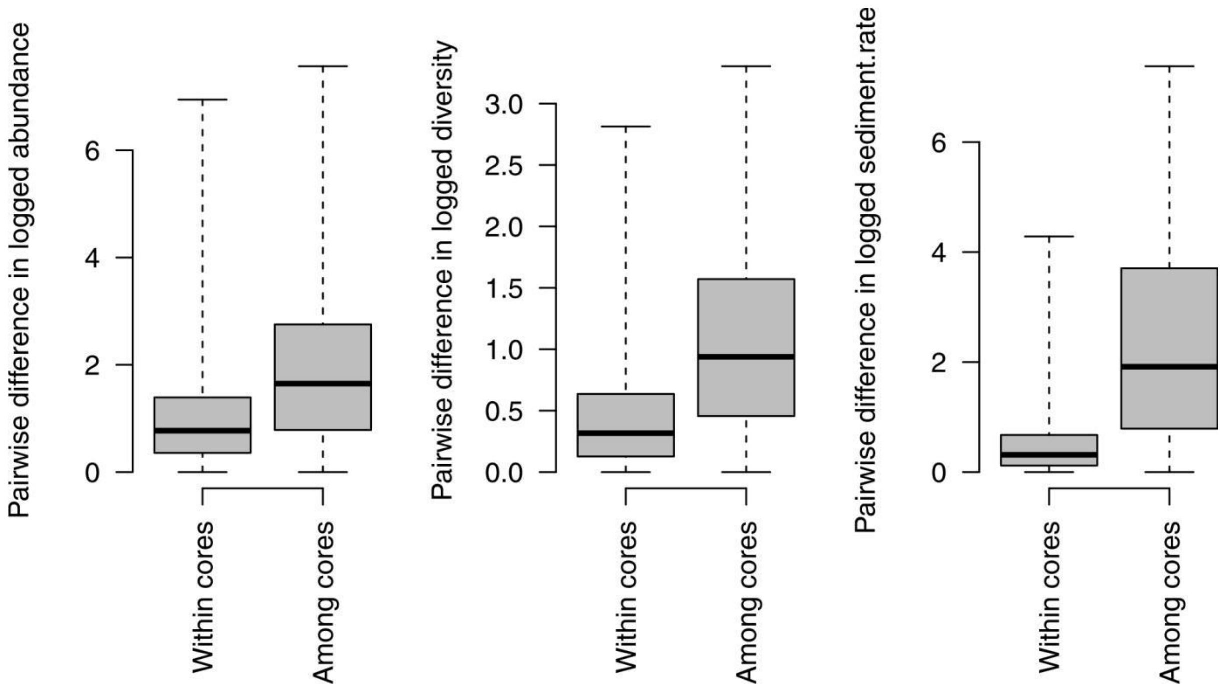

Figure S9. Variability in abundance, in diversity, and especially in sediment accumulation is markedly smaller within cores than among cores. Although some subset of cores from the Po coastal plain archive depositional conditions varying in sediment accumulation, the majority of cores in offshore environments were consistently deposited under low sediment accumulation.

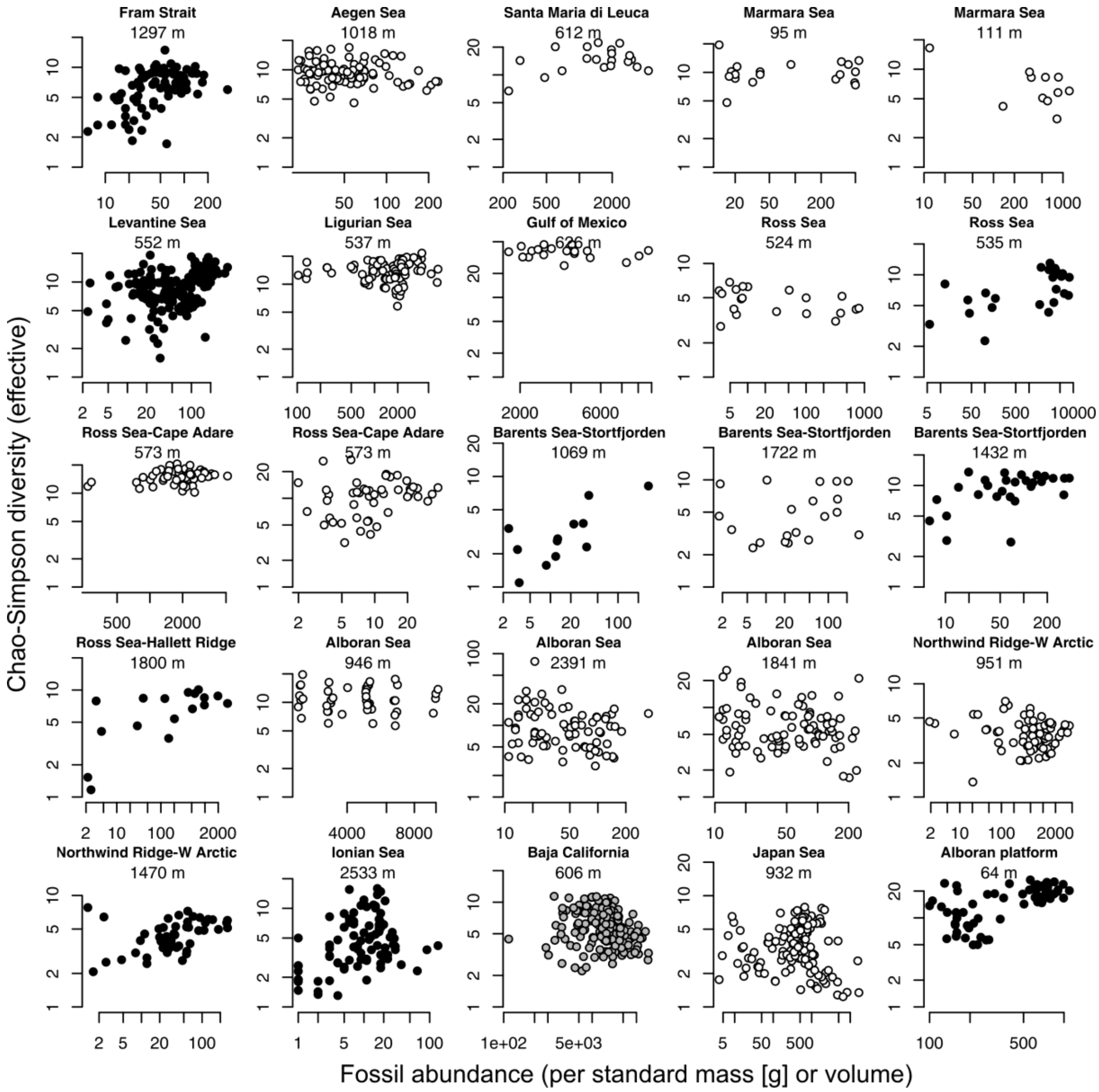

Figure S10. Local-scale (single-core) abundance-diversity relation in a selection of 25 microfossil datasets with benthic foraminifers, with mean sediment accumulation < 0.2 cm/y, coefficient variation in residence time > 0.25, coefficient variation in fossil abundance > 0.5, and gamma-level PIE-based diversity exceeding five species. 12 datasets show a significantly positive relation (black), one dataset shows a significantly negative relation (gray), and 12 datasets show insignificant relation (white). Data sources: Table S4.

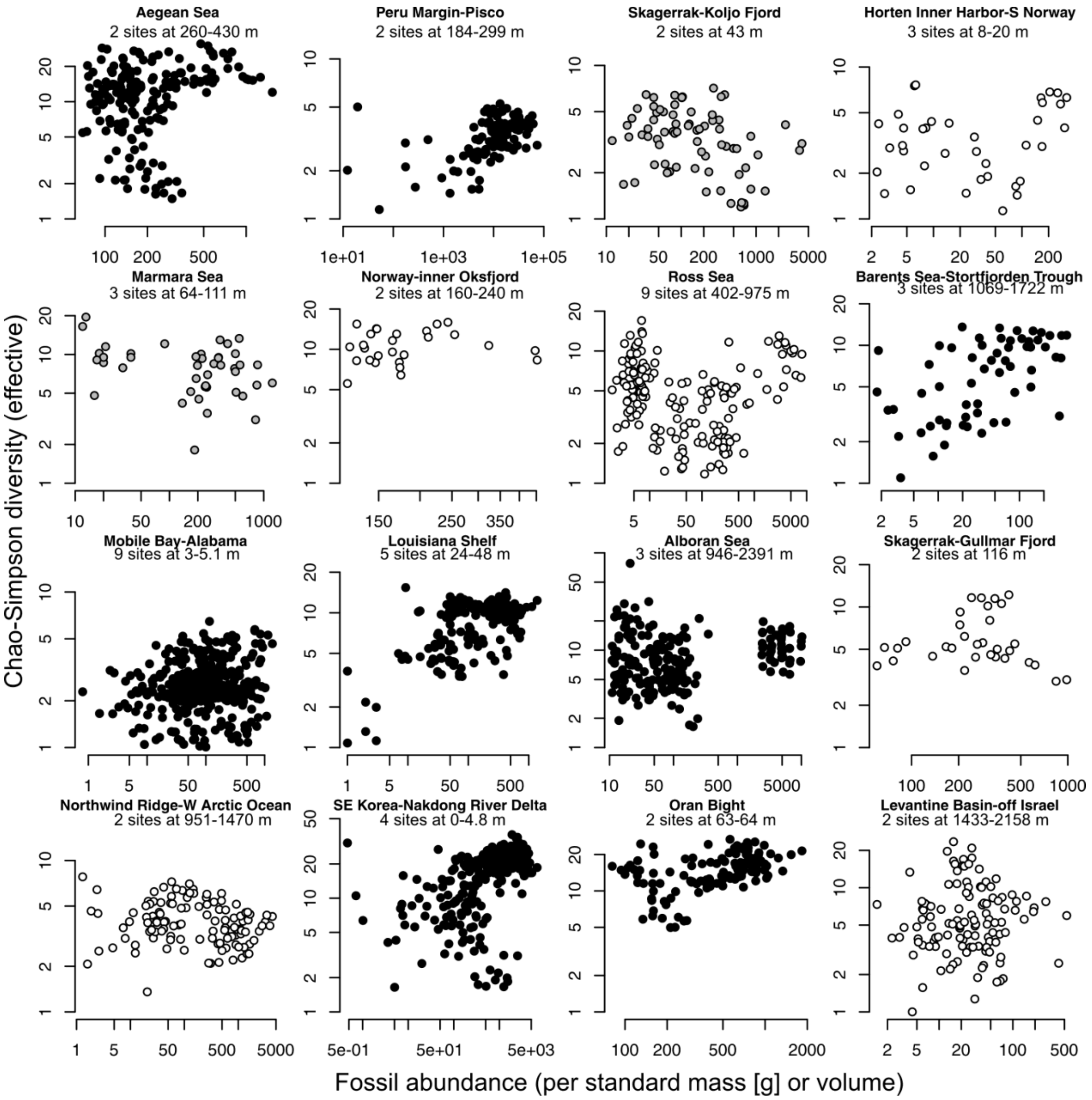

Figure S11. Regional-scale abundance-diversity relation in 16 microfossil datasets (at least two sites per region) with benthic foraminifers. 8 datasets show a significantly positive relation (black), six datasets show a significantly negative relation (gray), and two datasets show insignificant relation (white). Sources: Table S4.

Supporting tables

Table S1 – Diversity and abundance of living (non-averaged) molluscan assemblages in the northern Adriatic Sea, with source references. Data columns correspond to the reference, dataset ID (optional), latitude, longitude and water depth (m) of the assemblage, raw sample size and total abundance/m^2. Diversity indices correspond to the effective number of species based on the PIE-based and Simpson index, the effective number of species based on the Shannon index, and evenness values based on the Pielou J and Bulla O.

Table S2 – Diversity and abundance of fossil (time-averaged) molluscan assemblages collected in sediment cores in the northern Adriatic Sea. Individual fossil assemblages are in rows, data columns correspond to the core ID, sediment depth (cm), increment thickness (cm), systems tract (HST – highstand systems tract, MFZ – maximum flooding zone, TST – transgressive systems tract), facies association/environment, sediment accumulation (cm/y), sample size, fossil abundance/dm^3, Shannon H, Gini-Simpson index, Probability of interspecific encounter, the effective number of species (Simpson and PIE), evenness values based on the Pielou J and Bulla O, and the location of the assemblages along the first NMDS axis.

Table S3 - Abundance-diversity relations in 30 geographic datasets with benthic foraminiferal living assemblages (LADR), with references.

Table S4 – Abundance-diversity relations in 73 benthic foraminiferal fossil assemblages (FADR) in local stratigraphic series and in regional datasets, with references.

Table S5 – Input chronological data for Bacon function.

Supporting scripts

R language scripts for models and species-time relation

R language scripts for cartoons and data analyses

Supporting references – methods, age data, molluscan fossil assemblages

Amorosi, A., Centineo, M. C., Colalongo, M. L., Pasini, G., Sarti, G., and Vaiani, S.C. 2003. Facies architecture and latest Pleistocene–Holocene depositional history of the Po Delta

(Comacchio area), Italy. *Journal of Geology* 111, 39-56.

Amorosi, A., Bruno, L., Campo, B., Morelli, A., Rossi, V., Scarponi, D., Hong, W., Bohacs, K.M. and Drexler, T.M., 2017. Global sea-level control on local parasequence architecture from the Holocene record of the Po Plain, Italy. *Marine and Petroleum Geology* 87, 99-111.

Amorosi, A., Bruno, L., Campo, B., Costagli, B., Dinelli, E., Hong, W., Sammartino, I. and Vaiani, S.C., 2020. Tracing clinothem geometry and sediment pathways in the prograding Holocene Po Delta system through integrated core stratigraphy. Basin Research 32, 206-215.

Amorosi A., Bruno L., Campo B., Costagli B., Hong W., Picotti V., Vaiani S.C., 2021. Deformation patterns of upper Quaternary strata and their relation to active tectonics, Po Basin, Italy. *Sedimentology* 68, 402-424.

Berensmeier, M., Tomašových, A., Nawrot, R., Cassin, D., Zonta, R., Koubová, I. and Zuschin, M., 2023. Stratigraphic expression of the human impacts in condensed deposits of the Northern Adriatic Sea. *Geological Society, London, Special Publications* 529, 195-222.

Blaauw, M., Christen, J.A., Lopez, M.A.A., Vazquez, J.E., Belding, T., Theiler, J., Gough, B., Karney, C., Rcpp, L. and Blaauw, M.M., 2021. Package ‘rbacon’. Age-depth modelling using Bayesian statistics. Version: 3.1.1. https://CRAN.R-project.org/package=rbacon

Blaauw, M. and Christen, J.A., 2011. Flexible paleoclimate age-depth models using an autoregressive gamma process. *Bayesian Analysis* 6:457-474.

Bruno L., Bohacs K.M., Campo B., Drexler T.M., Rossi V., Sammartino I., Scarponi D., Hong, W., and Amorosi A. 2017. Early Holocene transgressive palaeogeography in the Po coastal plain (northern Italy). *Sedimentology* 64, 1792 - 1816

Bruno, L., Campo, B., Di Martino, A., Hong, W. and Amorosi, A. 2019. Peat layer accumulation and post-burial deformation during the mid-late Holocene in the Po coastal plain (Northern Italy). *Basin Research* 31, 621-639.

Calabrese L., Centineo M.C., Cibin U., Di Cocco I., 2009. Note Illustrative della Carta Geologica alla scala 1:50.000: Portomaggiore. *Servizio geologico sismico e dei suoli - Regione Emilia Romagna*, 98 pp.

Campo B., Bruno L., Amorosi A., 2020. Basin-scale stratigraphic correlation of late Pleistocene-Holocene (MIS 5e-MIS 1) strata across the rapidly subsiding Po Basin (northern

Italy). *Quaternary Science Reviews* 237, 106300.

Cheli A, Mancuso A, Azzarone M, Fermani S, Kaandorp J, Marin F, et al. 2021. Climate variation during the Holocene influenced the skeletal properties of Chamelea gallina shells in the North Adriatic Sea (Italy). *PLoS ONE* 16, e0247590.

Cibin U. et al., 2005 Note illustrative della Carta geologica d'Italia alla scala 1:50.00: Forlì-Cervia. *Servizio geologico sismico e dei suoli - Regione Emilia Romagna,* 104 pp.

Gallmetzer, I., Haselmair, A., Tomašových, A., Stachowitsch, M. and Zuschin, M., 2017. Responses of molluscan communities to centuries of human impact in the northern Adriatic Sea. *Plos One* 12, e0180820.

Gallmetzer, I., Haselmair, A., Tomašových, A., Mautner, A.K., Schnedl, S.M., Cassin, D., Zonta, R. and Zuschin, M., 2019. Tracing origin and collapse of Holocene benthic baseline communities in the northern Adriatic Sea. *Palaios* 34, 121-145.

Gouhier T.C. and Guichard F. 2014. Synchrony: quantifying variability in space and time. *Methods in Ecology and Evolution*, **5**, 524–533. R package version 0.3.8, http://synchrony.r-forge.r-project.org.

Haselmair, A., Gallmetzer, I., Tomašových, A., Wieser, A.M., Übelhör, A. and Zuschin, M., 2021. Basin-wide infaunalisation of benthic soft-bottom communities driven by anthropogenic habitat degradation in the northern Adriatic Sea. *Marine Ecology Progress Series* 671, 45-65.

Hsieh, T.C., Ma, K.H. and Chao, A., 2016. iNEXT: an R package for rarefaction and extrapolation of species diversity (H ill numbers). *Methods in Ecology and Evolution, 7*, 1451-1456.

Hubbell, S.P., 2001. The unified neutral theory of biodiversity and biogeography. *Princeton: Princeton University Press*.

Kidwell, S.M., 2002. Time-averaged molluscan death assemblages: palimpsests of richness, snapshots of abundance. *Geology, 30,* 803-806.

Lefcheck J.S. 2016. piecewiseSEM: Piecewise structural equation modeling in R for ecology, evolution, and systematics. *Methods in Ecology and Evolution,* **7**, 573-579.

Mautner, A.K., Gallmetzer, I., Haselmair, A., Schnedl, S.M., Tomašových, A. and Zuschin, M., 2018. Holocene ecosystem shifts and human-induced loss of Arca and Ostrea shell beds in the north-eastern Adriatic Sea. *Marine Pollution Bulletin* 126, 19-30.

Mazerolle M.J. 2023. AICcmodavg: Model selection and multimodel inference based on (Q)AIC(c). R package version 2.3.3, https://cran.r-project.org/package=AICcmodavg.

Mersmann, O., Trautmann, H., Steuer, D., and Bornkamp, B. 2018. truncnorm: Truncated Normal Distribution**.** Package 'truncnorm'. *R package version* 1.0-9. R (≥ 3.4.0), https://github.com/olafmersmann/truncnorm

Oksanen J., Blanchet G.F., Friendly M., Kindt R., Legendre P., McGlinn D., Minchin P.R., O'Hara B., Simpson G.L., Solymos P., Stevens M.H.H., Szoecs E. and Wagner H. 2020. vegan: Community Ecology Package. R package version 2.5-7. https://CRAN.R-project.org/package=vegan

Patil I., Makowski D., Ben-Shachar M., Wiernik B., Bacher E., and Lüdecke D. 2022. datawizard: An R Package for Easy Data Preparation and Statistical Transformations. *Journal of Open Source Software*, **7**, 4684. doi:10.21105/joss.04684.

Pinheiro J., Bates D., R Core Team 2023. *nlme: Linear and Nonlinear Mixed Effects Models*. R package version 3.1-164, https://CRAN.R-project.org/package=nlme.

Sarti G. et al., 2009 Note illustrative della Carta geologica d'Italia alla scala 1:50.00: Comacchio. Servizio geologico sismico e dei suoli - Regione Emilia Romagna, 126 pp.

Scarponi, D. and Kowalewski, M., 2004. Stratigraphic paleoecology: bathymetric signatures and sequence overprint of mollusk associations from upper Quaternary sequences of the Po Plain, Italy. *Geology*, *32*, 989-992.

Scarponi, D. and Kowalewski M. 2007. Sequence stratigraphic anatomy of diversity patterns: Late Quaternary benthic mollusks of the Po Plain, Italy. *Palaios*, *22*, 296-305.

Scarponi, D., Kaufman, D., Amorosi, A. and Kowalewski, M., 2013. Sequence stratigraphy and the resolution of the fossil record. *Geology* 41, 239-242.

Schnedl, S.M., Haselmair, A., Gallmetzer, I., Mautner, A.K., Tomašových, A. and Zuschin, M., 2018. Molluscan benthic communities at Brijuni Islands (northern Adriatic Sea) shaped by Holocene sea-level rise and recent human eutrophication and pollution. *Holocene* 28, 1801-1817.

Schumacker R.E., Lomax R.G. 2010. A beginner's guide to structural equation modelling. Routledge Taylor and Francis Group, 3rd Edition.

Severi et al., 2005. Note illustrative della Carta geologica d'Italia alla scala 1:50.00: Rimini. *Servizio geologico sismico e dei suoli - Regione Emilia Romagna*, 143 pp.

Tomašových, A., Gallmetzer, I., Haselmair, A., Kaufman, D.S., Vidović, J. and Zuschin, M., 2017. Stratigraphic unmixing reveals repeated hypoxia events over the past 500 yr in the northern Adriatic Sea. *Geology* 45, 363-366.

Tomašových, A., Gallmetzer, I., Haselmair, A., Kaufman, D.S., Kralj, M., Cassin, D., Zonta, R. and Zuschin, M., 2018. Tracing the effects of eutrophication on molluscan communities in sediment cores: outbreaks of an opportunistic species coincide with reduced bioturbation and high frequency of hypoxia in the Adriatic Sea. *Paleobiology* 44, 575-602.

Tomašových, A., Gallmetzer, I., Haselmair, A., Kaufman, D.S., Mavrič, B. and Zuschin, M., 2019. A decline in molluscan carbonate production driven by the loss of vegetated habitats encoded in the Holocene sedimentary record of the Gulf of Trieste. *Sedimentology* 66, 781-807.

Tomašových, A., Gallmetzer, I., Haselmair, A. and Zuschin, M., 2022. Inferring time averaging and hiatus durations in the stratigraphic record of high-frequency depositional sequences. *Sedimentology* 69, 1083-1118.

Wickham H. 2016. *ggplot2: Elegant Graphics for Data Analysis*. Springer-Verlag New York. ISBN 978-3-319-24277-4, https://ggplot2.tidyverse.org.

Wickham H., François R., Henry L., Müller K., and Vaughan D. 2023. *dplyr: A Grammar of Data Manipulation*. R package version 1.1.4, https://github.com/tidyverse/dplyr, https://dplyr.tidyverse.org.

Wood S.N. 2011. Fast stable restricted maximum likelihood and marginal likelihood estimation of semiparametric generalized linear models. *Journal of the Royal Statistical Society B*, **73**, 3-36.

Supporting references – living molluscan assemblages

Ambrogi, R. and Ambrogi, A.O., 1985. The estimation of secondary production of the marine bivalve *Spisula subtruncata* (da Costa) in the area of the Po River delta. *Marine Ecology* 6, 239-250.

Ambrogi, R., Colangelo, M.A., Fontana, P., Gatto, M., Sei, S. and Tracanella, E., 1995. La demografia del bivalve *Lentidium mediterraneum* nella zona di mare antistante il delta del Po. *Atti 6 congresso Società Italiana di Ecologia* 16, 165-167.

ARPAE 2010-2019. Valutazione dello stato delle acque marine costiere. Monitoraggio delle acque marino costiere e classificazione dello stato di qualità. *Regione Agenzia Prevenzione Ambiente Energia Emilia-Romagna*. https://www.arpae.it/it/temi-ambientali/mare/report-e-bollettini/stato-acque-marine

https://www.arpae.it/it/temi-ambientali/mare/report-e-bollettini/stato-acque-marine

Chiantore, M., Bedulli, D., Cattaneo-Vietti, R., Schiaparelli, S. and Albertelli, G., 2001. Long-term changes in the Mollusc-Echinoderm assemblages in the north and coastal middle Adriatic Sea. *Atti della Associazione Italiana di Oceanologia e Limnologia*, 14, 63-75.

ENEA. *Italian Mollusc Census Database of the Italian National Agency for New Technologies, Energy and Sustainable Economic Development*. http://www.santateresa.enea.it/wwwste/malaco/home.htm.

Forni, G. and Ambrogi, A.O., 2005. Struttura di popolazione del bivalve *Lentidium mediterraneum* e variazioni ambientali in Nord Adriatico. *Biologia Marina Mediterranea* 12, 277-280.

ISPRA (2012) Studio delle comunita' bentoniche. Monitoraggio del Terminale GNL – area della condotta offshore – Fase di esercizio provvisorio (2 E). *Istituto Superiore per la Protezione e la Ricerca Ambientale*.

Mavrič, B., Orlando-Bonaca, M., Bettoso, N. and Lipej, L., 2010. Soft-bottom macrozoobenthos of the southern part of the Gulf of Trieste: faunistic, biocoenotic and ecological survey. *Acta Adriatica* 51, 203-216.

Moodley, L., Heip, C.H. and Middelburg, J.J., 1998. Benthic activity in sediments of the northwestern Adriatic Sea: sediment oxygen consumption, macro-and meiofauna dynamics. *Journal of Sea Research 40*, 263-280.

N'Siala, G. M., V. Grandi, M. Iotti, G. Montanari, D. Prevedelli, and R. Simonini. 2008. Responses of a northern Adriatic Ampelisca–Corbula community to seasonality and short-term hydrological changes in the Po River. *Marine Environmental Research* 66, 466–476

Occhipinti-Ambrogi, A., Favruzzo, M. and Savini, D., 2002. Multi-annual variations of macrobenthos along the Emilia-Romagna Coast (Northern Adriatic). *Marine Ecology*, *23*, 307-319.

Orel, G., Marocco, R., Vio, E., Del Piero, D. and Della Seta, G., 1987. Sedimenti e biocenosi bentoniche tra la foce del Po ed il Golfo di Trieste (Alto Adriatico). *Bulletin d'Ecologie*, 18, 229-241.

Prevedelli, D., Simonini, R. and Ansaloni, I., 2001. Relationship of non-specific commensalism in the colonisation of the deep layers of sediment. *Journal of the Marine Biological Association of the United Kingdom* 81, 897-901.

Pitacco, V., Mistri, M., Aleffi, I.F., Lardicci, C., Prato, S., Tagliapietra, D. and Munari, C., 2019. Spatial patterns of macrobenthic alpha and beta diversity at different scales in Italian transitional waters (central Mediterranean). *Estuarine, Coastal and Shelf Science*, *222*, 126-138.

Poluzzi, A., Sabelli, B. and Taviani, M., 1981. Auto-sinecologia dei Molluschi: dei fondi mobili del delta settentrionale del Po (Estate 1980). *Bollettino della SocietaPaleontologica Italiana*, *21*, 169-178.

Rigotii, L. 2019. Studio e caratterizzazione preliminari di sedimento e macrozoobenthos in due stazioni marine costiere in località Ca' Roman (VE). *Dipartimento di Biologia, Universita' degli studi di Padova, Master thesis*.

Scardi, M., R. Crema, P. Di Dato, E. Fresi, and G. Orel. 2000. Le comunità bentoniche dell'Alto Adriatico: un'analisi preliminare dei cambiamenti strutturali dagli anni'30 ad oggi. Pp. 95–108 in O. Giovanardi, ed. Impact of trawl fishing on benthic communities. *Istituto Centrale per la Ricerca Scientifica e Tecnologica Applicata al Mare, Rome*.

Seneš, J., 1989. North Adriatic inter-island shelf ecosystems of the Rovinj area. *Geologica Carpathica* 40, 333-354.

Simonini, R., I. Ansaloni, A. B. Pagliai, and D. Prevedelli. 2004. Organic enrichment and structure of the macrozoobenthic community in the northern Adriatic Sea in an area facing Adige and Po mouths. *ICES Journal of Marine Science* 61, 871–881.

Solis-Weiss, V., Rossin, P., Aleffi, F., Bettoso, N., Orel, G., Vrišer, B., 2001. Gulf of Trieste: sensitivity areas using benthos and GIS techniques. In: Özhan, E. (Ed.), *Proceedings of the Fifth International Conference on the Mediterranean Coastal Environment*. Ankara, Turkey, 1567–1578. http://ipt.vliz.be/eurobis/resource?r=macroben_lbmrev_evco

Targusi, M. 2011. I crostacei Anfipodi quali descrittori delle comunità bentoniche di ambienti marino costieri interessati da attività antropiche. *Universita degli studi di Napoli Federico II, Dissertation thesis*.

Weber, K. and Zuschin, M., 2013. Delta-associated molluscan life and death assemblages in the northern Adriatic Sea: implications for paleoecology, regional diversity and conservation. *Palaeogeography, Palaeoclimatology, Palaeoecology, 370*, 77-91.

Zucchi Stolfa M.L. 1979. Lamellibranchi recenti delle lagune di Grado e di Marano. *Atti del Museo Friulano di Storia Naturale* 1, 41-60.

Zavodnik, D. and Vidakovic, J., 1987. Report on bottom fauna in two Northern Adriatic areas presumed to be influenced by inputs. *Report of the FAO/UNEP Meeting on the Effects of Pollution on Marine Ecosystems, Food and Agriculture Organization of the United Nations, Fisheries Report,* 352, Supplement, 263-279.

Supporting references – living benthic foraminiferal assemblages

Alves Martins, M.V., Hohenegger, J., Frontalini, F., Dias, J.M.A., Geraldes, M.C. and Rocha, F., 2019. Dissimilarity between living and dead benthic foraminiferal assemblages in the Aveiro Continental Shelf (Portugal). *PLoS One*, 14, e0209066.

Avnaim-Katav, S., Almogi-Labin, A., Kanari, M. and Herut, B., 2020. Living benthic foraminifera of southeastern Mediterranean ultra-oligotrophic shelf habitats: Implications for ecological studies. *Estuarine, Coastal and Shelf Science*, 234, 106633

Barras, C., Jorissen, F.J., Labrune, C., Andral, B. and Boissery, P., 2014. Live benthic foraminiferal faunas from the French Mediterranean Coast: Towards a new biotic index of environmental quality. *Ecological Indicators*, 36, 719-743.

Dimiza, M.D., Koukousioura, O., Triantaphyllou, M.V. and Dermitzakis, M.D., 2016. Live and dead benthic foraminiferal assemblages from coastal environments of the Aegean Sea (Greece): Distribution and diversity. *Revue de Micropaléontologie*, 59, 19-32

Dessandier, P.A., Bonnin, J., Kim, J.H. and Racine, C., 2018. Comparison of living and dead benthic foraminifera on the Portuguese margin: Understanding the taphonomical processes. *Marine Micropaleontology*, 140, 1-16

Diz, P. and Francés, G., 2008. Distribution of live benthic foraminifera in the Ría de Vigo (NW Spain). *Marine Micropaleontology*, 66, 165-191

Fentimen, R., Rüggeberg, A., Lim, A., Kateb, A.E., Foubert, A., Wheeler, A.J. and Spezzaferri, S., 2018. Benthic foraminifera in a deep-sea high-energy environment: the Moira Mounds (Porcupine Seabight, SW of Ireland). *Swiss Journal of Geosciences*, 111 561-572.

Harloff, J. and Mackensen, A., 1997. Recent benthic foraminiferal associations and ecology of the Scotia Sea and Argentine Basin. *Marine Micropaleontology*, 31, 1-29.

Jiang, F., Fan, D., Zhao, Q., Wu, Y., Ren, F., Liu, Y. and Li, A., 2023. Comparison of alive and dead benthic foraminiferal fauna off the Changjiang Estuary: Understanding water-mass properties and taphonomic processes. *Frontiers in Marine Science*, 10, 1114337.

Licari, L. and Mackensen, A., 2005. Benthic foraminifera off West Africa (1° N to 32° S): Do live assemblages from the topmost sediment reliably record environmental variability?. *Marine Micropaleontology*, 55, 205-233

Lutze, GF (1974): Benthische Foraminiferen in Oberflächen-Sedimenten des Persischen Golfes. Teil 1: Arten. *Meteor Forschungsergebnisse, Deutsche Forschungsgemeinschaft, Reihe C Geologie und Geophysik*, C17, 1-66

Mackensen, A., Fu, D.K., Grobe, H. and Schmiedl, G., 1993. Benthic foraminiferal assemblages from the eastern South Atlantic Polar Front region between 35 and 57 S: Distribution, ecology and fossilization potential. *Marine Micropaleontology*, 22, 33-69.

Mallon, J., Glock, N., and Schönfeld, J. 2012, The response of benthic foraminifera to low-oxygen conditions of the Peruvian oxygen minimum zone. *In: Altenbach, A., Bernhard J.M. and Seckbach J., eds, Anoxia: Evidence for Eukaryote Survival and Paleontological Strategies,* Springer, Dordrecht, 305–321.

In: ANOXIA :. , ed. by Altenbach, Alexander V., Bernhard, Joan M. and Seckbach, Joseph. Cellular Origin, Life in Extreme Habitats and Astrobiology, 21

Martins, M.V.A., Hohenegger, J., Frontalini, F., Miranda, P., da Conceição Rodrigues, M.A. and Dias, J.M.A., 2016. Comparison between the dead and living benthic foraminiferal assemblages in Aveiro Lagoon (Portugal). *Palaeogeography, Palaeoclimatology, Palaeoecology,* 455, 16-32.

Martins, M.V.A., Hohenegger, J., Martínez-Colón, M., Frontalini, F., Bergamashi, S., Laut, L., Belart, P., Mahiques, M., Pereira, E., Rodrigues, R. and Terroso, D., 2020. Ecological quality status of the NE sector of the Guanabara Bay (Brazil): A case of living benthic foraminiferal resilience. *Marine Pollution Bulletin*, 158, 111449

Melis, R. and Violanti, D., 2006. Foraminiferal biodiversity and Holocene evolution of the Phetchaburi coastal area (Thailand Gulf). *Marine Micropaleontology*, 61, 94-115.

Mojtahid, M., Jorissen, F., Lansard, B., Fontanier, C., Bombled, B. and Rabouille, C., 2009. Spatial distribution of live benthic foraminifera in the Rhône prodelta: Faunal response to a continental–marine organic matter gradient. *Marine Micropaleontology*, 70, 177-200

Oron, S., Friedlander, A.M., Sala, E. and Goodman-Tchernov, B.N., 2022. Recent shallow water foraminifera from the Selvagens Islands (Northeast Atlantic)–Assemblage composition and biogeographic significance. *Estuarine, Coastal and Shelf Science*, 264, 107671

Parent, B., Barras, C., Bicchi, E., Charrieau, L.M., Choquel, C., Bénéteau, É., Maillet, G.M. and Jorissen, F.J., 2021. Comparison of four foraminiferal biotic indices assessing the environmental quality of coastal Mediterranean soft bottoms. *Water*, 13, 3193

Raposo, D., Frontalini, F., Clemente, I., da Conceição Guerreiro Couto, E., Veríssimo, F. and Laut, L., 2022. Benthic foraminiferal response to trace elements in a tropical mesotidal Brazilian estuary. *Estuaries and Coasts*, 45, 2610-2631

Schmidt, S. and Schönfeld, J., 2021. Living and dead foraminiferal assemblage from the supratidal sand Japsand, North Frisian Wadden Sea: distributional patterns and controlling factors. *Helgoland Marine Research*, 75, 6, 1-22

Schumacher, S., Jorissen, F.J., Dissard, D., Larkin, K.E. and Gooday, A.J., 2007. Live (Rose Bengal stained) and dead benthic foraminifera from the oxygen minimum zone of the Pakistan continental margin (Arabian Sea). *Marine Micropaleontology*, 62, 45-73

Szarek, R., Kuhnt, W., Kawamura, H. and Kitazato, H., 2006. Distribution of recent benthic foraminifera on the Sunda Shelf (South China Sea). Marine Micropaleontology, 61, 171-195

Thies, A., 1991. Die Benthos-Foraminiferen im Europäischen Nordmeer. *Doctoral dissertation, Christian-Albrechts-Universität Kiel.*

Timm, S., 1992. Rezente Tiefsee-Benthosforaminiferen aus Oberflächensedimenten des Golfes von Guinea (Westafrika)-Taxonomie, Verbreitung, Ökologie und Korngrößenfraktionen. *Doctoral dissertation, Geologisch-Paläontologisches Institut und Museum Christian-Albrechts-Universität Kiel.*

Venturelli, R.A., Rathburn, A.E., Burkett, A.M. and Ziebis, W., 2018. Epifaunal foraminifera in an infaunal World: Insights into the influence of heterogeneity on the benthic ecology of oxygen-poor, deep-sea habitats. *Frontiers in Marine Science,* 5, 344.

Walton, W.R., 1955. Ecology of living benthonic foraminifera, Todos Santos Bay, Baja California. *Journal of Paleontology,* 29, 952-1018.

Wollenburg, J.E. and Mackensen, A., 1998. Living benthic foraminifers from the central Arctic Ocean: faunal composition, standing stock and diversity. *Marine Micropaleontology*, 34, 153-185

Supporting references – fossil benthic foraminiferal assemblages

Abu-Zied, R.H., Rohling, E.J., Jorissen, F.J., Fontanier, C., Casford, J.S. and Cooke, S., 2008. Benthic foraminiferal response to changes in bottom-water oxygenation and organic carbon flux in the eastern Mediterranean during LGM to Recent times. *Marine Micropaleontology*, 67, 46-68.

Avnaim-Katav, S., Almogi-Labin, A., Schneider-Mor, A., Crouvi, O., Burke, A.A., Kremenetski, K.V. and MacDonald, G.M., 2019. A multi-proxy shallow marine record for Mid-to-Late Holocene climate variability, Thera eruptions and cultural change in the Eastern Mediterranean. *Quaternary Science Reviews*, 204, 133-148.

Buzas-Stephens, P., Livsey, D.N., Simms, A.R. and Buzas, M.A., 2014. Estuarine foraminifera record Holocene stratigraphic changes and Holocene climate changes in ENSO and the North American monsoon: Baffin Bay, Texas. *Palaeogeography, Palaeoclimatology, Palaeoecology*, 404, 44-56.

Cardiff J. et al. 2019. Multidecadal Changes in Marine Subsurface Oxygenation Off Central Peru During the Last ca. 170 Years. *Frontiers in Marine Science*, 10.3389/fmars.2019.00270.

Consolaro, C., Rasmussen, T.L. and Panieri, G., 2018. Palaeoceanographic and environmental changes in the eastern Fram Strait during the last 14,000 years based on benthic and planktonic foraminifera. *Marine Micropaleontology*, 139, 84-101.

Dimiza, M.D., Fatourou, M., Arabas, A., Panagiotopoulos, I., Gogou, A., Kouli, K., Parinos, C., Rousakis, G. and Triantaphyllou, M.V., 2020. Deep-sea benthic foraminifera record of the last 1500 years in the North Aegean Trough (northeastern Mediterranean): A paleoclimatic reconstruction scenario. *Deep Sea Research Part II: Topical Studies in Oceanography*, 171, 104705.

Filipsson, H.L. and Nordberg, K., 2004. A 200-year environmental record of a low-oxygen fjord, Sweden, elucidated by benthic foraminifera, sediment characteristics and hydrographic data. *Journal of Foraminiferal Research*, 34, 277-293.

Fink, H.G; Wienberg, C.; Hebbeln, D.; McGregor, H.V.; Schmiedl, G.; Taviani, M.; Freiwald, A. (2012): Oxygen control on Holocene cold-water coral development in the eastern Mediterranean Sea. *Deep Sea Research Part I: Oceanographic Research Papers*, 62, 89-96

Hess, S., Alve, E., Andersen, T.J. and Joranger, T., 2020. Defining ecological reference conditions in naturally stressed environments–How difficult is it? *Marine Environmental Research*, 156, 104885.

Kaminski, M.A., Aksu, A., Box, M., Hiscott, R.N., Filipescu, S. and Al-Salameen, M., 2002. Late Glacial to Holocene benthic foraminifera in the Marmara Sea: implications for Black

Sea–Mediterranean Sea connections following the last deglaciation. *Marine Geology*, 190, 165-202.

Klootwijk, A.T., Alve, E., Hess, S., Renaud, P.E., S?rlie, C. and Dolven, J.K., 2021. Monitoring environmental impacts of fish farms: Comparing reference conditions of sediment geochemistry and benthic foraminifera with the present. *Ecological Indicators*, 120, 106818.

Le Houedec, S., Mojtahid, M., Bicchi, E., de Lange, G.J. and Hennekam, R., 2020. Suborbital hydrological variability inferred from coupled benthic and planktic foraminiferal?based proxies in the southeastern Mediterranean during the last 19 ka. *Paleoceanography and Paleoclimatology*, 35, e2019PA003827.

Matos, L., Wienberg, C., Titschack, J., Schmiedl, G., Frank, N., Abrantes, F., Cunha, M.R. and Hebbeln, D., 2017. Coral mound development at the Campeche cold-water coral province, southern Gulf of Mexico: Implications of Antarctic Intermediate Water increased influence during interglacials. *Marine Geology*, 392, 53-65.

Melis, R. and Salvi, G., 2009. Late Quaternary foraminiferal assemblages from western Ross Sea (Antarctica) in relation to the main glacial and marine lithofacies. *Marine Micropaleontology*, 70, 39-53.

Melis, R. and Salvi, G., 2020. Foraminifer and Ostracod Occurrence in a Cool-Water Carbonate Factory of the Cape Adare (Ross Sea, Antarctica): A Key Lecture for the Climatic and Oceanographic Variations in the Last 30,000 Years. *Geosciences*, 10, 413.

Melis, R., Capotondi, L., Torricella, F., Ferretti, P., Geniram, A., Hong, J.K., Kuhn, G., Khim, B.K., Kim, S., Malinverno, E. and Yoo, K.C., 2021. Last Glacial Maximum to Holocene paleoceanography of the northwestern Ross Sea inferred from sediment core geochemistry and micropaleontology at Hallett Ridge. *Journal of Micropalaeontology*, 40, 15-35.

Melis, R., Carbonara, K., Villa, G., Morigi, C., Bárcena, M.A., Giorgetti, G., Caburlotto, A., Rebesco, M. and Lucchi, R.G., 2018. A new multi?proxy investigation of Late Quaternary palaeoenvironments along the north-western Barents Sea (Storfjorden Trough Mouth Fan). *Journal of Quaternary Science*, 33, 662-676.

Milker, Y., Schmiedl, G. and Betzler, C., 2011. Paleobathymetric history of the Western Mediterranean Sea shelf during the latest glacial period and the Holocene: Quantitative reconstructions based on foraminiferal transfer functions. *Palaeogeography, Palaeoclimatology, Palaeoecology*, 307, 324-338.

Mojtahid, M., Toucanne, S., Fentimen, R., Barras, C., Le Houedec, S., Soulet, G., Bourillet, J.F. and Michel, E., 2017. Changes in northeast Atlantic hydrology during Termination 1: Insights from Celtic margin's benthic foraminifera. *Quaternary Science Reviews*, 175, 45-59.

Osterman, L.E. and Smith, C.G., 2012. Over 100 years of environmental change recorded by foraminifers and sediments in Mobile Bay, Alabama, Gulf of Mexico, USA. *Estuarine, Coastal and Shelf Science*, 115, 345-358.

Osterman, L.E., Pavich, K., and Caplan, J., 2004, Benthic foraminiferal census data from Gulf of Mexico cores (Texas and Louisiana Continental Shelf). *U.S. Geological Survey Open-File Report* 2001-1209, 15 p.

Pérez-Asensio, J.N., Frigola, J., Pena, L.D., Sierro, F.J., Reguera, M.I., Rodríguez-Tovar, F.J., Dorador, J., Asioli, A., Kuhlmann, J., Huhn, K. and Cacho, I., 2020. Changes in western Mediterranean thermohaline circulation in association with a deglacial Organic Rich Layer formation in the Alboran Sea. *Quaternary Science Reviews*, 228, 106075.

Pinto, A.F.S., Martins, M.V.A., Fonseca, M.C.M., Pereira, E., Terroso, D.L., Rocha, F., Rodrigues, M.A.C., 2017. Late Holocene closure of a barrier beach in Sepetiba Bay and its environmental impact (Rio de Janeiro, Brazil). *Journal of Sedimentary Environments*, 2, 65-80.

Polovodova Asteman, I. and Nordberg, K., 2013. Foraminiferal fauna from a deep basin in Gullmar Fjord: The influence of seasonal hypoxia and North Atlantic Oscillation. *Journal of Sea Research*, 79, 40-49.

Polyak, L., Best, K.M., Crawford, K.A., Council, E.A. and St-Onge, G., 2013. Quaternary history of sea ice in the western Arctic Ocean based on foraminifera. *Quaternary Science Reviews*, 79, 145-156.

Richwine, K.A., Marot, M., Smith, C.G., Osterman, L.E. and Adams, C.S., 2013. Biological and geochemical data of gravity cores from mobile Bay, Alabama. *US Department of the Interior, US Geological Survey*.

Schmiedl, G., Hemleben, C., Keller, J. and Segl, M., 1998. Impact of climatic changes on the benthic foraminiferal fauna in the Ionian Sea during the last 330, 0000 years. *Paleoceanography*, 13, 447-458.

Schmiedl, G., Mitschele, A., Beck, S., Emeis, K.C., Hemleben, C., Schulz, H., Sperling, M. and Weldeab, S., 2003. Benthic foraminiferal record of ecosystem variability in the eastern Mediterranean Sea during times of sapropel S5 and S6 deposition. *Palaeogeography, Palaeoclimatology, Palaeoecology*, 190, 139-164.

Takata, H., Hong, S.H., Yoo, D.G., Kim, J.C., Cheong, D. and Khim, B.K., 2022. Fossil benthic foraminifera in the Nakdong River Delta (southeast Korea) during the early to middle Holocene. *Paleontological Research*, 26, 283-300.

Tetard, M., Licari, L. and Beaufort, L., 2017. Oxygen history off Baja California over the last 80 kyr: A new foraminiferal?based record. *Paleoceanography*, 32, 246-264.

Tsujimoto, A., Nomura, R., Yasuhara, M., Yamazaki, H. and Yoshikawa, S., 2006. Impact of eutrophication on shallow marine benthic foraminifers over the last 150 years in Osaka Bay, Japan. *Marine Micropaleontology*, 60, 258-268.

Usami, K., Ohi, T., Hasegawa, S. and Ikehara, K., 2013. Foraminiferal records of bottom-water oxygenation and surface-water productivity in the southern Japan Sea during 160–15 ka: associations with insolation changes. *Marine Micropaleontology*, 101, 10-27.

Xiang, R., Yang, Z., Saito, Y., Fan, D., Chen, M., Guo, Z. and Chen, Z., 2008. Paleoenvironmental changes during the last 8400 years in the southern Yellow Sea: Benthic foraminiferal and stable isotopic evidence. *Marine Micropaleontology*, 67, 104-119.